PRODUCTION OF PRECIPITATED CALCIUM CARBONATE FROM MARBLE WASTE BY CALCINATION-HYDRATION-CARBONATION

A THESIS SUBMITTED TO
THE GRADUATE SCHOOL OF NATURAL AND APPLIED SCIENCES
OF
MIDDLE EAST TECHNICAL UNIVERSITY

BY

HAZAL MELİS BAYDAR

IN PARTIAL FULFILLMENT OF THE REQUIREMENTS
FOR
THE DEGREE OF MASTER OF SCIENCE
IN
MINING ENGINEERING

FEBRUARY 2022

Approval of the thesis:

PRODUCTION OF PRECIPITATED CALCIUM CARBONATE FROM MARBLE WASTE BY CALCINATION-HYDRATION-CARBONATION

submitted by **HAZAL MELİS BAYDAR** in partial fulfillment of the requirements for the degree of **Master of Science** i**n Mining Engineering, Middle East Technical University** by,

Prof. Dr. Halil Kalıpçılar
Dean, Graduate School of **Natural and Applied Sciences** _____

Prof. Dr. Naci Emre Altun
Head of the Department, **Mining Engineering, METU** _____

Prof. Dr. Ali İhsan Arol
Supervisor, **Mining Engineering, METU** _____

Examining Committee Members:

Prof. Dr. Naci Emre Altun
Mining Engineering, METU _____

Prof. Dr. Ali İhsan Arol
Mining Engineering, METU _____

Assoc. Prof. Dr. İlkay Bengü Can
Mining Engineering, Hacettepe University _____

Date: 03.02.2022

I hereby declare that all information in this document has been obtained and presented in accordance with academic rules and ethical conduct. I also declare that, as required by these rules and conduct, I have fully cited and referenced all material and results that are not original to this work.

Name Last name : Hazal Melis Baydar

Signature :

ABSTRACT

PRODUCTION OF PRECIPITATED CALCIUM CARBONATE FROM MARBLE WASTE BY CALCINATION-HYDRATION-CARBONATION

Baydar, Hazal Melis
Master of Science, Mining Engineering
Supervisor: Prof. Dr. Ali İhsan Arol

February 2022, 81 pages

Precipitated calcium carbonate (PCC) is used as a filler and extender in many different industries, particularly in paint, paper, plastic, adhesive, and sealant. Today, high purity limestone is preferred as a raw material for PCC production. In this study, it is aimed to use marble waste as an alternative raw material, which has nearly the same chemical composition as limestone. In this regard, the possibility of recycling the marble waste to produce PCC, a product with added value, was investigated. In the study, PCC production was carried out by the carbonation method, which includes the stages of calcination of stones, slaking of lime with distilled water, and carbonation of milk of lime with CO_2. During the production stages, differences between limestone and marble waste were tried to be observed by using limestone as a reference raw material. The optimum calcination conditions were examined at calcination temperature values of 900, 950, and 1000°C for particle size intervals of -25.4+12.7 mm and -12.7+6.35 mm in varying calcination times for marble waste and limestone. As a result of the calcination experiments, it was observed that there was no difference between marble waste and limestone in terms of calcination efficiency. 20 minutes at 1000°C, after reaching the desired temperature with the

preheating rate of 15°C/minute, was found to be sufficient to achieve a calcination efficiency of 98% and higher for both particle size intervals. In the hydration of lime experiments, varying lime to water ratios (1:3.5, 1:4.0, and 1:4.5) were examined to observe the reactivity of limes by monitoring the temperature increase during the process. It was observed that the reactivity of lime of marble origin was similar to lime of limestone origin, considering increases in temperature profiles. Carbonation experiments were carried out by using $Ca(OH)_2$ concentrations of 5% and 10% at CO_2 pressures of 5 and 10 bar. It was seen that PCCs produced from marble origin have almost the same particle size distributions as PCCs produced from limestone under the same precipitation conditions. The morphology of the produced PCCs was observed as rhombohedral. The result of experiments indicates that marble waste could be an alternative raw material instead of limestone for the precipitated calcium carbonate production.

Keywords: Precipitated Calcium Carbonate (PCC), Marble Waste, Calcination, Carbonation, Recycling

ÖZ

MERMER ATIKLARINDAN KALSİNASYON-SÖNDÜRME-KARBONATLAMA YÖNTEMİ İLE ÇÖKTÜRÜLMÜŞ KALSİYUM KARBONAT ÜRETİMİ

Baydar, Hazal Melis
Yüksek Lisans, Maden Mühendisliği
Tez Yöneticisi: Prof. Dr. Ali İhsan Arol

Şubat 2022, 81 sayfa

Çökeltilmiş kalsiyum karbonat (ÇKK), boya, kağıt, plastik, yapıştırıcı ve dolgu macunu başta olmak üzere birçok farklı endüstride dolgu maddesi olarak kullanılmaktadır. Günümüzde PCC üretimi için hammadde olarak yüksek saflıkta kireçtaşı tercih edilmektedir. Bu çalışmada, kireçtaşı ile neredeyse aynı kimyasal bileşime sahip mermer atıklarının alternatif hammadde olarak kullanılması amaçlanmıştır. Bu kapsamda mermer atıklarının geri kazanılarak katma değere sahip bir ürün olan PCC'nin üretilebilme olasılığı araştırılmıştır. Çalışmada, PCC üretimi, kalsinasyon, kirecin distile su ile söndürülmesi ve kireç sütünün CO_2 ile karbonatlama aşamalarını içeren karbonasyon yöntemi ile gerçekleştirilmiştir. Üretim aşamalarında, kireçtaşı referans hammadde olarak kullanılarak, kireçtaşı ve mermer atığı arasındaki farklılıklar gözlemlenmeye çalışılmıştır. Mermer atığı ve kalker için değişen kalsinasyon sürelerinde -25.4+12.7 mm ve -12.7+6.35 mm tane boyutu aralıkları için 900, 950 ve 1000°C kalsinasyon sıcaklık değerlerinde optimum kalsinasyon koşulları incelenmiştir. Kalsinasyon deneyleri sonucunda mermer atığı ile kalker arasında kalsinasyon verimi açısından bir fark olmadığı gözlemlenmiştir.

15°C/dakikalık ön ısıtma hızı ile istenilen sıcaklığa ulaştıktan sonra 1000°C'de 20 dakika, her iki partikül boyutu aralığı için %98 ve daha yüksek bir kalsinasyon verimi elde etmek için yeterli bulunmuştur. Kireç hidratasyonu deneylerinde, işlem sırasında sıcaklık artışını izleyerek kireçlerin reaktivitesini gözlemlemek için değişen kireç-su oranları (1:3.5, 1:4.0 ve 1:4.5) incelenmiştir. Sıcaklık profillerindeki artışlar dikkate alındığında, mermer kökenli kirecin reaktivitesinin kalker kökenli kirecinkine benzer olduğu gözlenmiştir. Karbonatlama deneyleri, 5 ve 10 bar CO_2 basınçlarında, %5 ve %10 $Ca(OH)_2$ konsantrasyonları kullanılarak gerçekleştirilmiştir. It was seen that PCCs produced from marble origin have almost the same particle size distributions as PCCs produced from limestone under the same precipitation conditions. Üretilen PCC'lerin morfolojisi eşkenar dörtgen olarak gözlenmiştir. Deneylerin sonucu, çökeltilmiş kalsiyum karbonat üretimi için mermer atıklarının kalker yerine alternatif bir hammadde olabileceğini göstermektedir.

Anahtar Kelimeler: Çöktürülmüş Kalsiyum Karbonat (PCC), Mermer Atıkları, Kalsinasyon, Karbonasyon, Geri Dönüşüm

To My Family and Friends

ACKNOWLEDGMENTS

I would like to express my sincerest thankfulness to my advisor Prof. Dr. Ali İhsan Arol, for his valuable supervision, encouragement, and insight. He guided me whenever I needed his advice, allowing me to find my own way through this learning process. I would also like to thank my examining committee members, Prof. Dr. Naci Emre Altun and Doç. Dr. İlkay Bengü Can for their valuable comments and criticism. I want to extend my thanks to Abdülvahit Torun for his contributions throughout this study.

I would like to thank İsmail Kaya, Aytekin Arslan, and Caner Baytar for their technical support during my laboratory works.

The Turkish Cement Manufacturers' Association R&D Institute is gratefully acknowledged for the analyses and suggestions.

I am thankful to my colleague Aslı Ulusoy Tasar for her support and motivation. I am particularly indebted to my dear friends Gizem Aslan, Şahin Furkan Şahiner, Zafer Demirtaş, and Gaye Baştürk Ayaz for their valuable friendship, support and endless patience, whenever I needed to them.

Finally, I am deeply grateful to my grandfather Yusuf Saldamlı, my grandmother Kadriye Saldamlı, my mother Aynur Saldamlı, my aunt Hatice Saldamlı, and my cousin Berfin Arslan for their endless support and encouragement throughout my education life. I want to express my special thanks to Şahabettin Mert Aytaç for his endless support and precious insight during my hard times.

TABLE OF CONTENTS

APPENDICES

LIST OF TABLES

TABLES

LIST OF FIGURES

FIGURES

CHAPTER 1

INTRODUCTION

1.1 Background

Turkey being one of the oldest marble producers in the world, has great marble reserves due to its geological location and structure. In the world, marble reserves are mainly located in countries such as Greece, Iran, Italy, Portugal, Spain, Turkey, and Pakistan, which are in the Alpine-Himalayan belt (Karahan, 2018). In Turkey, most of the marble reserves are concentrated in Western Anatolia and Thrace. Menteşe, Menderes, Kazdağ and Istıranca Massifs in Western Anatolia, Kırşehir in Central Anatolia, Bitlis Massif in Eastern Anatolia, Elazığ and its surroundings have rich in marble deposits (Ketin, 1984). Afyonkarahisar, Balıkesir, Bilecik, Bursa, Denizli, Eskişehir, Muğla, Uşak, Kırklareli and Kırşehir are the provinces where the majority of marble reserves with various colors, patterns and qualities are located in Turkey (Çetin, 2003).Throughout history, marbles have been used by mankind as a building stone or in artistic activities in parallel with the development and progress of civilization. The first evaluations of marble reserves in Turkey were made in 1966 by the General Directorate of Mineral Research and Exploration of Turkey (MTA). According to MTA report, the total amounts of marble reserves are estimated as approximately 5,1 billion m^3 (13,9 billion tonnes) in Turkey, shown in Table 1.1.

Table 1.1 Total marble reserves in Turkey (MTA,1966)

Reserves	Cubic Meter (m^3)	Metric ton (tonne)
Measured Reserves	589,000,000	1,590,000,000
Probable Reserves	1,545,000,000	4,171,000,000
Possible Reserves	3,027,000,000	8,172,000,000
Total	5,161,000,000	13,934,000,000

In Turkey, the private sector is in charge of marble production. In the Turkish marble sector, it is estimated that there are 2,821 marble quarries, 2,000 factories, 9,000 workshops, and 300,000 employees (Karahan, 2018). According to MAPEG mine production statistics, annual marble production in Turkey is given in Figure 1.1 between years 2011 and 2020. Approximately 10.7 million tonnes of marble was produced in 2020.

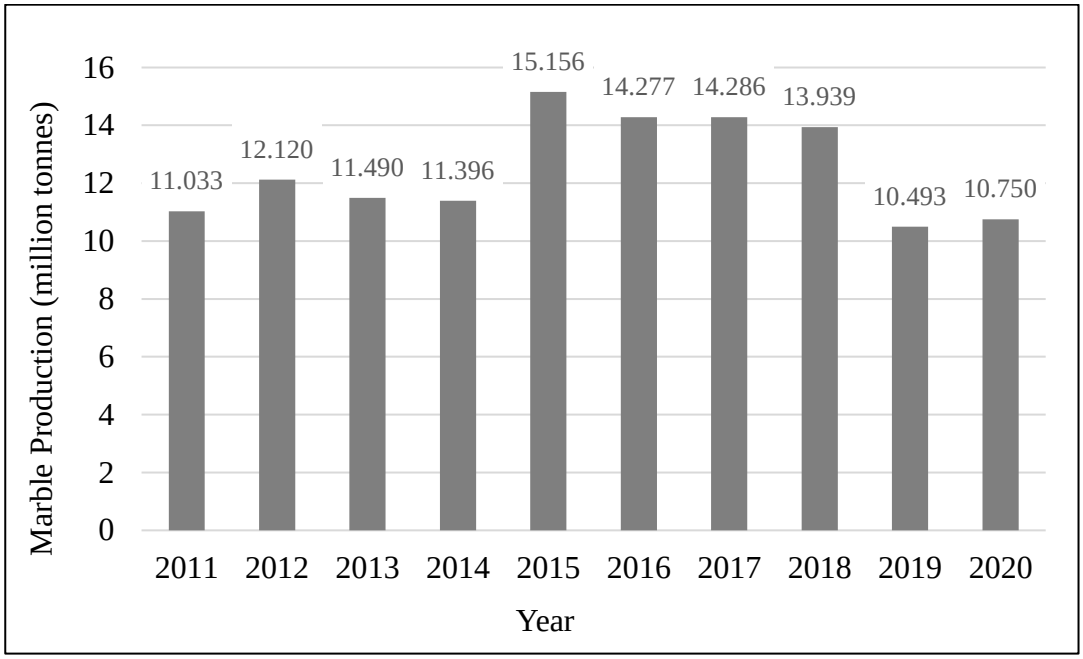

Figure 1.1 Marble production in Turkey between years 2011 and 2020 (MAPEG, 2020)

The mining method is determined based on the geographical and topological characteristics of the deposit and economic factors. In the world, marble deposits could be exploited with the surface (mainly) and underground mining methods. In Turkey, marble is extracted by quarrying, which is one of the surface mining methods (MEGEP, 2008). In the quarries, marble production could be broadly divided into two main stages: extracting and processing marble blocks. In the extraction stage, marble is cut into blocks using the mechanized equipment after necessary drilling operations. Over time, block cutting made with human power has

been replaced by mechanical parts and machines such as diamond wire saws and armed-chain cutting machines.

In quarrying operations, cutting, trimming, and shaping blocks produce a large amount of waste. The removal of overburden and the development of benches, roads, and ramps are the other source of waste generation. Additionally, the presence of natural cracks and faults in the marble blocks and changes in geotechnical features of the quarry leads to an increase in waste generation. The sizes of these wastes vary from small pieces to large blocks as well as fine dust particles produced from the cutting and drilling operations.

In the processing stage, marble blocks extracted from parent rock are subjected to processing operations in plants unless sold in blocks. Gangsaw and S/T machines are used for the preparation of the desired size of marble products. During the processing of blocks, cutting, slabbing, sizing, and polishing (optional) operations contribute to waste generation in the form of small pieces, chips, and slurry or semi-slurry (Mehta et al., 2020b).

A considerable amount of marble wastes of various sizes and shapes are generated during the quarrying and processing operations. For the purpose of utilization of marble wastes, many practical applications were examined in various fields of industry. Marble wastes could be used in aggregate production, in the road and embankment construction, in manufacturing of concrete, bricks, and ceramic in addition to substitute raw material for limestone in various industries such as cement, paper, paint, and plastic. Additionally, fine marble powder with high calcite is used in the rehabilitation of acidic soils, in the production of antiacid drugs in the field of pharmacy, and feed industry to increase egg production. Apart from these, the production of high purity precipitated calcium carbonate (PCC) has the potential to utilize marble waste. On the other hand, it is important to produce PCC in accordance with the standards for the industries in which they will be used (Bilgin & Koç, 2013; Mehta et al., 2020b).

1.2 Statement of the Problem

Waste management is becoming a crucial practice for long-term sustainability all over the world, which aims to conserve natural resources, promote environmental sustainability, prevent pollution and save energy (EPA, 2020). In this context, waste management is essential to reduce the adverse effects of marble waste on the environment and health since marble mining activities produce a large amount of waste materials. There are several studies about the amount of waste generated during marble production all over the world. In the Custonaci Industrial Zone in Sicily, which has 15.7% of the marble production of Italy and 2.7% of the world production, only 25% of marble production is used commercially, with the remaining 75% being an industrial waste (Liguori et al., 2008). In Pakistan, it is reported that the total estimated waste is at the level of 74-85% in the marble quarries that produce blocks by the conventional blasting method (World Bank, 2006). In Greece, it has been calculated that the average recovery rate in a marble quarry does not exceed 15%, based on the annual production and waste amounts (Grossou-Yalta et al., 2003). In India, it is estimated that roughly 30-40% of the total marble extracted in mechanized quarries is waste. This rate reaches 60-70% in quarries that produce marble with conventional blasting methods (Mehta et al., 2020a). In Afyon-Iscehisar, Turkey, 40-60% of the overall marble block production in the extraction stage is discarded as waste, on average (Çelik, 1996). By examining 18 natural stone processing plants in Torbalı, İzmir, the amount of marble waste generated in the marble processing plants that produce marble using gang saw and S/T machines has been calculated as 40% of the total amount of stone extracted from the quarries. (Elçi et al., 2017).

The variety in the size of the marble waste, the amount of waste, and the meager recycling rate impose additional costs to companies in the storage and disposal of these wastes. Although marble wastes are categorized as inert waste, these wastes create environmental problems in the dumpsite (Kun, 2013).

There are several impacts of marble wastes on the environment. Uncontrolled storage of marble waste causes an unsightly and unaesthetic appearance in nature as well as topography alteration and land occupation. In addition, these waste materials have the potential to destroy vegetation by negatively affecting soil fertility. Dust formation is another critical problem associated with marble waste. Fine or ultrafine-sized marble wastes mixed with the air adversely affect the breathable air quality. Besides, marble waste in the dust form can lead to degradation of surface and groundwater quality (Bilgin & Koç, 2013; Karaca et al., 2012; Mehta et al., 2020b).

Figure 1.2 Marble waste generated mainly by the mining activities

1.3 Objectives and Scope of the Study

The objective of this study is to produce precipitated calcium carbonate (PCC) from the marble waste by calcination, hydration, and carbonation. The study aims to eliminate the adverse effects (land occupation, unaesthetic appearance, etc.) of marble wastes generated from mining activities and the processing of marble blocks. It also aims to manage marble wastes in a possibly effective way in quarries by

recycling. For these purposes, the production of PCC, which is an added value product, could be an essential practice in waste management.

Within the scope of the study, marble waste and limestone (as a reference) were used as raw materials in PCC production. PCCs were synthesized by the carbonation route which is an industrial production method including calcination, hydration of lime followed by slaking of lime, and carbonation stages. The PCCs were synthesized under the same conditions to compare them. Throughout the study, the products obtained at the end of each production stage from marble waste and limestone were examined, and the detected differences were tried to be revealed.

The main stages of the research are described as follows;

(i) Characterization of the marble waste and limestone, including mineralogical, chemical, and thermal analyses.

(ii) Investigation of the calcination efficiencies of marble waste and limestone samples in varying temperature, time, and particle size ranges.

(iii) Determination of optimum parameter levels for the calcination experiments.

(iv) Investigation of the temperature profile of the hydration reaction for marble waste and limestone in varying lime to water ratios.

(v) Investigation of the particle size distribution of PCCs obtained at the carbonation process under varying CO_2 pressure and $Ca(OH)_2$ concentrations.

(vi) Characterization of the PCCs produced from marble waste and limestone, including mineralogical, morphological, and color analyses.

CHAPTER 2

THEORY AND LITERATURE REVIEW

2.1 Limestone

2.1.1 Definition and Origin of Limestone

Carbonate sedimentary rocks are estimated to constitute nearly 20-25% of all sedimentary rocks (Boggs, 2009). By definition, carbonate rocks should be composed of more than 50% carbonate minerals which are mainly calcite ($CaCO_3$), aragonite ($CaCO_3$), and dolomite ($Ca.Mg(CO_3)_2$). According to the mineral composition, these rocks are broadly divided into two major types: limestone and dolostone, which is also known as dolomite rock. Whereas dolostone is composed of calcium magnesium carbonate, limestone consists primarily of calcium carbonate as the main mineral composition (Tucker, 2001).

Calcium, which is a chemical component of calcium carbonate, is the fifth most common element in the earth's crust. Calcium was extracted from early igneous rocks through both weathering of rocks and the leaching effects of acidic gases such as carbon dioxide, oxides of sulfur, or nitrogen, which are dissolved in rainwater. The sedimentary deposition of calcium carbonate ($CaCO_3$), which was later converted into naturally occurring limestone rock, was formed as a result of the reaction between calcium ions and carbon dioxide dissolved in sea or freshwater (Oates, 1998).

It is possible to identify the formation of limestones as three processes: (i) precipitation (or crystallization) of calcium carbonate by organic and inorganic or combination of both organic and inorganic processes, (ii) lithification of carbonate sediments, and (iii) replacement of some other minerals by calcium carbonate.

Marine, shallow-water, marginal marine, and nonmarine environments are the major carbonate deposition areas (Sanders & Friedman, 1967). The commercially viable deposits of limestones are commonly sedimented by organic routes that include a wide variety of organisms such as gastropods, bivalves, foraminifera, corals, sponges, and algae that have existed in the marine environment. While some of these organisms are able to build their shells or skeletons using calcium carbonate dissolved in seawater, some of them have the ability to secrete calcium carbonate. Some of the biogenic carbonate sediments are also produced in nonmarine environments such as lakes, streams, and alluvial fans. However, carbonate deposits that are formed inland waters are generally not of economic importance compared to those produced in the marine environment. On the other hand, inorganic precipitation of carbonates has the potential to produce economically significant deposits such as travertine and oolitic limestone, which occur either in the marine environment or inland waters (Oates, 1998).

2.1.2 Mineral Composition of Limestone

As a mineral composition, limestones might be composed of calcite (chiefly), aragonite, magnesite, and dolomite minerals without any impurities. The physical properties of these carbonate minerals are given in Table 2.1 (Boynton, 1980).

Table 2.1 The main physical properties of carbonate minerals

Carbonate Minerals	**Formula**	**Molecular weight (g/mol)**	**Crystal System**	**Specific Gravity (g/cm^3)**	**Hardness (Mohs)**
Calcite	$CaCO_3$	100.1	rhombohedral	2.72	3
Aragonite	$CaCO_3$	100.1	orthorhombic	2.94	3.5-4
Magnesite	$MgCO_3$	84.3	rhombohedral	3	3.5-4.5
Dolomite	$Ca.Mg(CO_3)_2$	184.4	rhombohedral	2.83	3.5-4

The crystalline polymorphs of calcium carbonate are formed depending on the precipitation conditions such as pH, saturation, the temperature of the solution as well as the presence of inorganic ions (Jimoh et al., 2018; Domingo et al., 2006). Calcite, aragonite, and vaterite are the three polymorphs of calcium carbonate in an anhydrite form. Some distinct crystallographic and lattice parameters of these polymorphs are shown in Table 2.2. The thermodynamically most stable polymorph of calcium carbonate is the calcite which crystallizes a rhombohedral lattice system. Naturally occurring aragonite is less stable than calcite and exhibits need like morphology. Vaterite is the unstable polymorph of calcium carbonate and rarely forms at ambient temperature and pressure conditions, so it tends to transform into calcite or aragonite in nature (Boynton, 1980; Koutsoukos & Chen, 2010).

Table 2.2 Crystallographic and lattice parameters of calcium carbonate polymorphs (Belete, 2019; Koutsoukos & Chen, 2010)

Parameters	Calcite	Aragonite	Vaterite
Crystal System	Trigonal (Hexagonal-rhombohedral)	Orthorhombic	Hexagonal
Crystal Morphology	Cubic to rhombohedral	Needle like or elongated prisms	Spherical or disklike
Lattice Parameters	a = b = 4.9880 Å c = 17.0610 Å	a = 4.9616 Å b = 7.9705 Å c = 5.7394 Å	a = b = 4.1304 Å c = 8.4749 Å
Unit cell	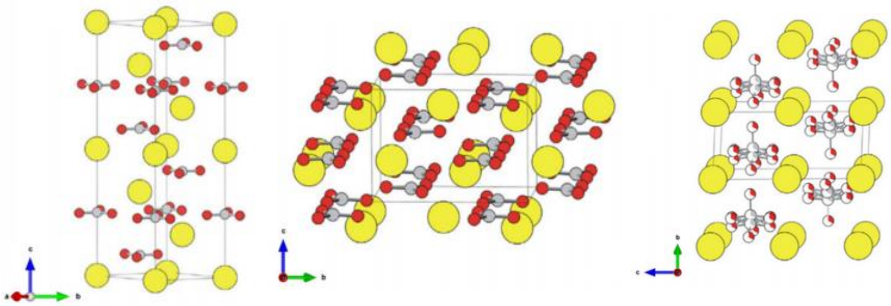		

2.1.3 Impurities

Limestones have a wide variety of physical and chemical properties depending on formation route, diagenesis, depositional environment, and impurities. Limestone contains different levels of impurities and trace elements which affect the selection of suitable limestones for many applications. Impurities could be concentrated or disseminated during the deposition and following diagenesis of limestones. Basically, impurities could be classified as homogeneous and heterogeneous. Silica and alumina originating from clay, silt, and sand are the major impurities that could be either homogeneously disseminated in the stone in the early stages of deposition or concentrated in the faults and bedding planes as heterogenous impurities. Iron is distributed in the limestone either homogeneously in the form of iron carbonate or heterogeneously in the form of pyrite, limonite, hematite, and magnetite. Sulfates are the source of sulfur, a homogeneous impurity found in the limestone. Homogeneously distributed carbon is derived from organic residues. In limestone production, washing, screening, and selective quarrying are the common methods to remove heterogeneous impurities from the limestones. On the other hand, it is not possible to avoid homogeneous impurities by using these methods. The remaining impurities are trace elements due to the low concentration levels. Only a limited number of deposits with trace elements such as silver and mercury are of economic importance (Boynton, 1980; Oates, 1998). According to Murray's (1954) study, the levels of trace elements and impurities present in the American limestones with high calcium content are summarised in Table 2.3.

Table 2.3 Impurities and trace elements in limestone (Oates, 1998)

Impurities and Trace elements	**Typical Range**	**Units**
Silica (SiO_2)	0.1-2	%
Iron (Fe_2O_3)	0.02-0.6	%
Alumina (Al_2O_3)	0.04-1.5	%

Table 2.3 (continued)

Sulfur ($CaSO_4$)	0.01-0.5	%
Carbonaceous matter	0.01-0.5	%
Manganese (MnO_2)	20-1000	mg/kg
Antimony (Sb)	0.1-3	mg/kg
Arsenic (As)	0.1-15	mg/kg
Boron (B)	1-20	mg/kg
Copper (Cu)	1-30	mg/kg
Lead (Pb)	0.5-30	mg/kg
Mercury (Hg)	0.02-0.1	mg/kg
Molybdenum (Mo)	0.1-4	mg/kg
Nickel (Ni)	0.5-15	mg/kg
Silver (Ag)	0.2-4	mg/kg
Tin (Sn)	0.1-15	mg/kg
Zinc (Zn)	3-500	mg/kg

The levels and types of impurities have a great influence on the colors of limestone. Deposits with high purity commonly have a white color, whereas most conventional deposits have a gray or tan color. Limestones that contain carbonaceous material or iron sulfides could be shades of gray or black color, while the presence of traces of iron and manganese gives the limestone yellow, cream, and red colors (Boynton, 1980).

It is possible to classify limestones based on different properties such as type, average grain size, texture, and principle impurities. In addition to these, the carbonate content plays an important role in selecting a suitable deposit for the desired end-products. The purity classification of limestone-based on calcium carbonate content was devised by Cox et al. (1977). The purity classification extended by adding magnesia, silica, and iron oxide as quality criteria (Mitchell, 2011). The extended purity classification of limestone is presented in Table 2.4.

Table 2.4 Purity classification of limestone by calcium carbonate content (Mitchell, 2011)

Purity Classification	$CaCO_3$ (wt.%)	CaO (wt.%)	MgO (wt.%)	SiO_2 (wt.%)	Fe_2O_3 (wt.%)
Very high purity	>98.5	>55.2	<0.8	<0.2	<0.05
High purity	97.0-98.5	54.3-55.2	0.8-1.0	0.2-0.6	0.05-0.1
Medium purity	93.5-97.0	52.4-54.3	1.0-3.0	0.6-1.0	0.1-1.0
Low purity	85.0-93.5	47.6-52.4	>3.0	<2.0	>1.0
Impure	<85.0	<47.6	>3.0	>2.0	>1.0

2.1.4 Industrial Use of Limestones

Limestone has been extensively used in various industries in the form of crushed limestone, ground calcium carbonate (GCC), or precipitated calcium carbonate (PCC). The limestone applications are summarized in the following (Oates, 1998).

Construction and Building: The main usage of limestone in the construction and building industries is as crushed rock. The limestone aggregates and filler is used in concrete and roadstone depending on the particle shape and crushing strength. Sand for mortar, filter media, rip rap, and armour stone for sea defense are the other common applications of limestone.

Cement: Limestone (with low-magnesium preferred) is a raw material for cement manufacturing. A wide variety of physical and chemical properties could be acceptable if the magnesium carbonate content does not exceed 5% of the calcium carbonate content.

Agriculture: To increase the pH of acidic soils, ground limestone is extensively utilized. It is also used to minimize the effects of acid rains. Furthermore, fertilizer formulation includes limestone in small amounts in addition to animal feed.

Metal Refining: Limestone is used as a fluxing agent in metal smelting. In blast furnaces, limestone is utilized to eliminate impurities as molten slag. Limestone may also be used to make slags in steelmaking and to extract bauxite for aluminum production.

Quicklime Production: Limestone is a raw material to produce quicklime that has significant uses areas in many industries. Quicklime is a product of limestone decomposition at high temperatures.

Acid Gas Removal: Limestone is used as an absorbent reacting with acidic gases such as SO_2, SO_3, HCl, and HF to reduce emissions.

Other Uses: Precipitated calcium carbonate (PCC) is used in paint, paper, plastic, printing inks, toothpaste, rubber, and sealings as fillers and extenders. Also, limestone has several applications in water treatment, sewage filtration, and effluent neutralization. It is also used in the glass and ceramics industries as a raw material.

2.2 Marble

2.2.1 Definition and Origin of Marble

As a geological definition, marble is a metamorphic rock formed by the recrystallization of limestone and dolostone under the influence of pressure and temperature (Leontakianakos et al., 2013). Before the metamorphism, limestone/dolostone was an aggregation of separate particles cemented into a rock mass. During the process of metamorphism, the noncrystalline limestone or dolostone grains re-form into a marble rock consisting of equigranular crystals. At the early phases of the transformation, calcium carbonate ($CaCO_3$) crystals are relatively small. As metamorphism progress, the crystals become larger and more recognizable as the intergrown crystal form of calcium carbonate ($CaCO_3$). As a result of these processes, the sedimentary structure and texture of the original limestone/dolostone rock have been changed permanently (Bowles, 1916).

2.2.2 Mineral Composition of Marble

During the process of metamorphism, limestone undergoes physical and chemical changes in mineral assemblage and texture variation and forms marble. This process generally includes textural and mineralogical changes.

Marble is almost entirely composed of calcium and/or magnesium carbonates without impurities. A calcite marble could be consist of 96-99% calcium carbonate ($CaCO_3$), whereas a dolomite marble/dolomarble contains approximately 54% calcium carbonate ($CaCO_3$) and 46% magnesium carbonate ($MgCO_3$) (Bowles, 1916; Boynton, 1980).

2.2.3 Impurities

The common impurities present in the marble are listed as silica (SiO_2), iron oxides (FeO and Fe_2O_3), manganese oxide (MnO), alumina (Al_2O_3), and sulfur. The less common impurities with a small amount are titanium, sodium, lithium, and phosphorus oxides as well as organic matters. Additionally, there are mineral impurities in marble in the form of grains. Quartz, hematite, graphite, pyrite, biotite, muscovite, talc, and mica could be regarded as the common mineral impurities in marble (Bowles, 1916; Karahan, 2018).

The color, which is the most distinctive physical property of the marble, is governed by the mineral constituents present in it. Generally, the black and grayish shades are due to the presence of fine graphite grains in marble. Red, pink, and reddish-brown shades are to be attributed to manganese oxides (MnO, Mn_2O_3) or to hematite (Fe_2O_3). Also, the grains of the hydrous oxide of iron and limonite ($2Fe_2O_3.3H_2O$) cause yellow-brown, yellow, or cream colors (Bowles, 1916).

Afyon White, Muğla White, Elazığ Cherry, Bilecik Pink, Burdur Beige, and Ege Rose are well-known Turkish marbles that are classified based on color in international markets (Karahan, 2018).

2.2.4 Industrial Use of Marble

The main consumption areas of marble are the construction industry, the field of fine arts, and decoration. The most significant usage area is the construction sector. Interior and exterior coverings of buildings, decoration works, monuments, sculptures, ornaments, and souvenirs are important consumption areas.

It is increasingly used in road and paving, curbstone, wall construction, wall covering, stair step, roof covering,, landscaping, garden stepping stone, indoor flooring, kitchen, bathrooms, interior and exterior decoration (Karahan, 2018).

2.3 Precipitated Calcium Carbonate (PCC)

The precipitated calcium carbonate (PCC), also known as purified or synthetic calcium carbonate, is the fine or very fine calcium carbonate nanoparticle produced from high purity carbonate rocks. The commercial PCCs are made in three processes: (i) calcination of carbonate rocks, (ii) hydration of limes, followed by the obtaining milk of lime, and (iii) carbonation of milk of limes (Minerals Technologies Inc., 2021). Additionally, ground calcium carbonate (GCC) has been used in the cement and construction industries for several years. GCC is produced by grinding calcium carbonate rocks without any chemical reaction. Although PCC and GCC have the same chemical composition, PCC is purer than the GCC with lower silica, magnesium, and lead content. The crystal morphology of GCC is an irregular shape of rhombohedral particles, whereas the PCC morphology is a uniform shape of calcite polymorphs compared to the GCC crystals (Jimoh et al., 2018; Mantilaka et al., 2013; Chen & Nan, 2011). The particle size distribution of PCC is more uniform than GCC, so it provides smoothness and low abrasion properties to the products (El-Sherbiny et al., 2015). Moreover, PCCs with high internal porosity and a higher specific area provide an effective chemical absorption and binding efficiency (D'Haese et al., 2013). The brightness, opacity, and purity properties of PCCs are better than GCCs (Hubbe and Gill, 2016).

2.3.1 Precipitated Calcium Carbonate (PCC) Production

The precipitated calcium carbonate has been produced commercially since 1841. English company John E. Sturge Ltd., which is the first producer of commercial PCC, treated calcium chloride ($CaCl_2$) obtained as a by-product in the potassium chlorate ($KClO_3$) process with soda ash (Na_2CO_3) and carbon dioxide (CO_2). In 1898, a new factory was built to produce PCC using the milk of lime process by the same company (Minerals Technologies Inc., 2021).

Depending on the precipitation conditions and routes that are conducted in the PCC production, the different types of calcium carbonate polymorphs could be achieved. The common methods for the precipitation of calcium carbonate are given in Figure 2.1 schematically (Domingo et al., 2006). By using these methods, PCCs in fine or very fine nanoparticle size could be produced.

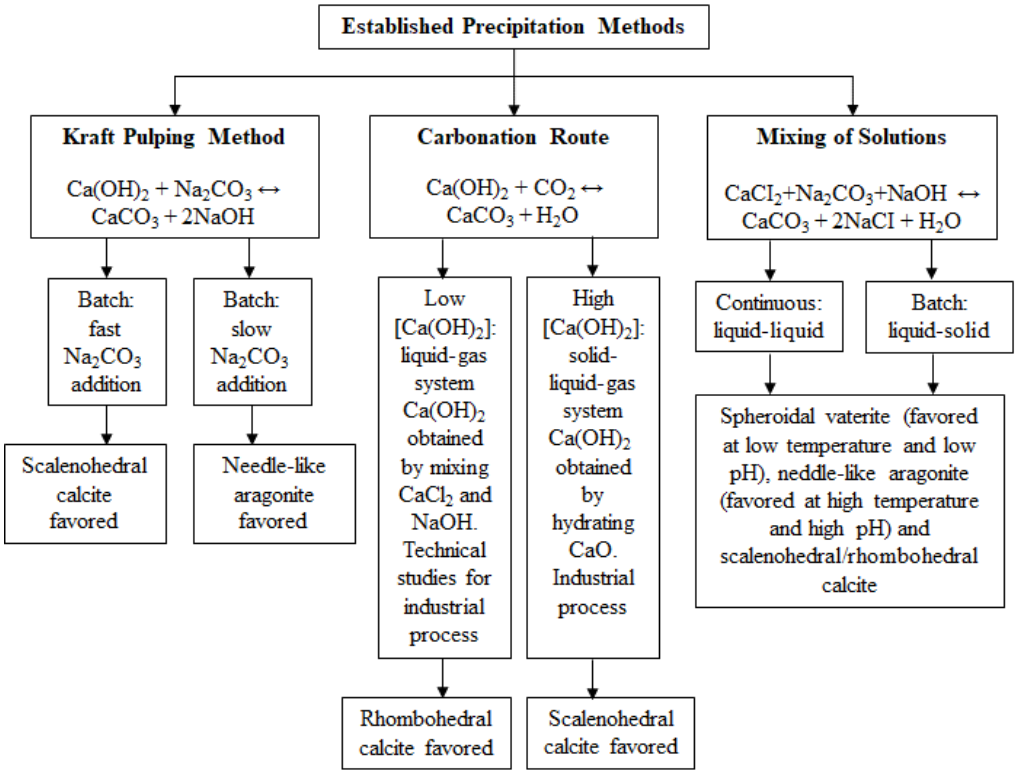

Figure 2.1 Established precipitation methods in the production of PCCs (Domingo et al., 2006)

In the Kraft pulping method, the PCCs are produced as a by-product from the causticizing process which is used for the industrial production of sodium hydroxide (NaOH). The rate of soda ash (Na_2CO_3) addition to calcium hydroxide ($Ca(OH)_2$) determines whether the product will be calcite or aragonite. Secondly, PCCs are also obtained by using a method of mixing solutions containing calcium (Ca^{+2}) and carbonate (CO_3^{-2}) ions in an aqueous solution, particularly for laboratory research. By using a mixture of solutions in batch or continuous process, calcite, aragonite, or vaterite are produced. The carbonation is the other most common industrial production route of the PCCs with the bubbling carbon dioxide (CO_2) through calcium hydroxide ($Ca(OH)_2$) (Domingo et al., 2006).

Several alternative sources have been examined to produce precipitated calcium carbonate. Teir et al. (2005) used calcium silicates ($CaSiO_3$) as a raw material in the production of PCC to eliminate the carbon dioxide (CO_2) emission released during the calcination process of the carbonates. Teir et al. (2007) investigated the PCC production from iron and steel slags, which dissolve in acetic acid to save energy and decrease carbon dioxide (CO_2) emissions. The possibility of PCC production from fly ashes was studied by Dogan and Yıldırım (2008). Chukwudebelu et al. (2013) investigated the recovery of pure slaked lime from automobile welders' carbide sludge using solubilization and evaporation processes. In addition to these alternative sources, there are several studies related to the utilization of marble waste. The usability of marble waste in concrete production was studied by Hebhoub et al. (2011). The possibility of marble waste dust utilization as an additive in industrial brick production was investigated by Bilgin et al. (2012). Altun (2016) studied the possibility of marble wastes utilization in wet flue gas desulphurization. The precipitated calcium carbonate production from waste marble powder was also investigated by Erdoğan and Eken (2017).

Through the study, the carbonation route with a solid-liquid-gas system is going to be used as the production method of precipitated calcium carbonate from marble waste. The main stages of this industrial production of PCC from limestone are illustrated in Figure 2.2.

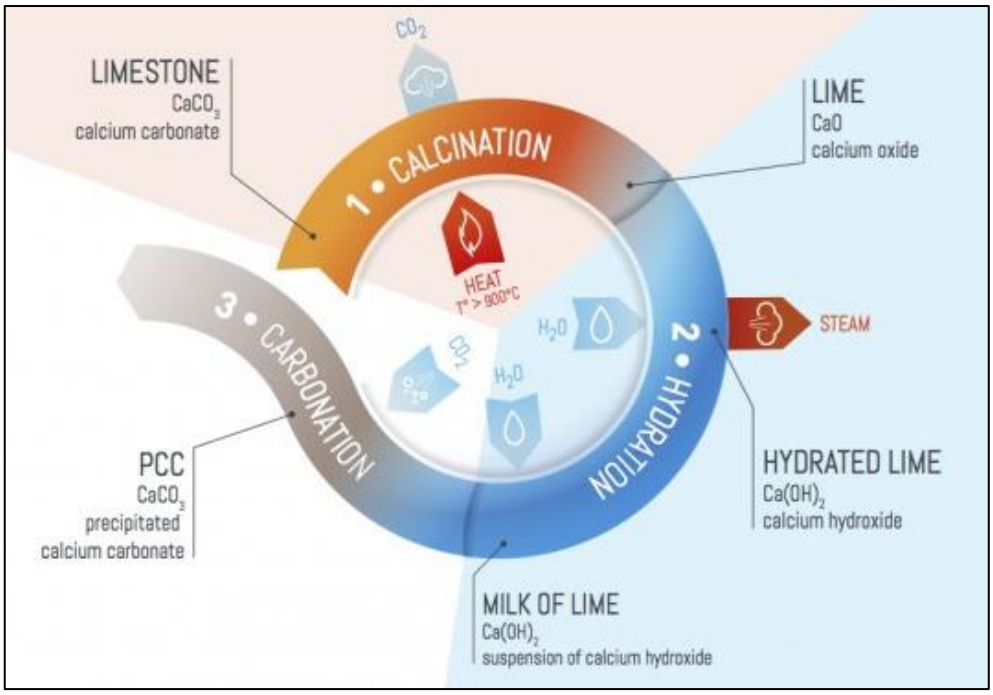

Figure 2.2 Stages of PCC production with carbonation route (Lhoist Group, n.d.)

2.3.1.1 Calcination of Limestone

The term 'calcination' was originated from the Latin word 'calcinare' which means to burn lime. Calcination or calcining is defined as a process of heating a substance below its melting point, causing a physical or chemical change such as loss of moisture, oxidization or reduction, and thermal decomposition of compounds in the absence of air, or a limited supply of air or oxygen. Calcination operations have been extensively used for the purposes of heat treatment for phase transformation, removal of water from hydrates, carbon dioxide from carbonates and other bounded gases from ores or petroleum coke, impurities from minerals (Oates, 1998).

In the calcination of limestone, calcium carbonate mineral is decomposed into calcium oxide, which is also known as quicklime, burned lime or unslaked lime, and carbon dioxide by heating, which is expressed as follows (Teir et al., 2005):

$$CaCO_{3(s)} + \text{Heat} \rightarrow CaO_{(s)} + CO_{2(g)}, \qquad \Delta H_{(\text{at } 1000^{\circ}C)} = 165.54 \text{ kJ/mol} \quad (2.1)$$

In commercial calcination operations, reactions occur at high temperatures in order to meet the high heat demand since the reactions are endothermic. The decomposition temperature associated with the partial pressure of the carbon dioxide could be observed in Figure 2.3 for the calcium carbonate (Chorney, 2019).

According to Figure 2.3, the dissociation temperature of calcium carbonate ($CaCO_3$) is approximately 900°C, in which the CO_2 partial pressure reaches a value of 1 atm in a 100% CO_2 atmosphere. The dissociation temperature of magnesium carbonate ($MgCO_3$) is between 402 and 550°C at 1 atm. in a 100% CO_2 atmosphere. Since dolomitic/magnesian limestone rocks contain different proportions of $CaCO_3$ and $MgCO_3$, their dissolution temperature also varies from 510 to 750°C. The differences in the crystallinity of these limestones also affect the dissociation temperature. In addition, the impurities present in the carbonate rocks affect the decomposition temperature. In practice, calcination temperatures of carbonate rocks are considerably higher than their theoretical values because the reaction and heat transfer rates are not rapid enough for economical operation (Boynton, 1980).

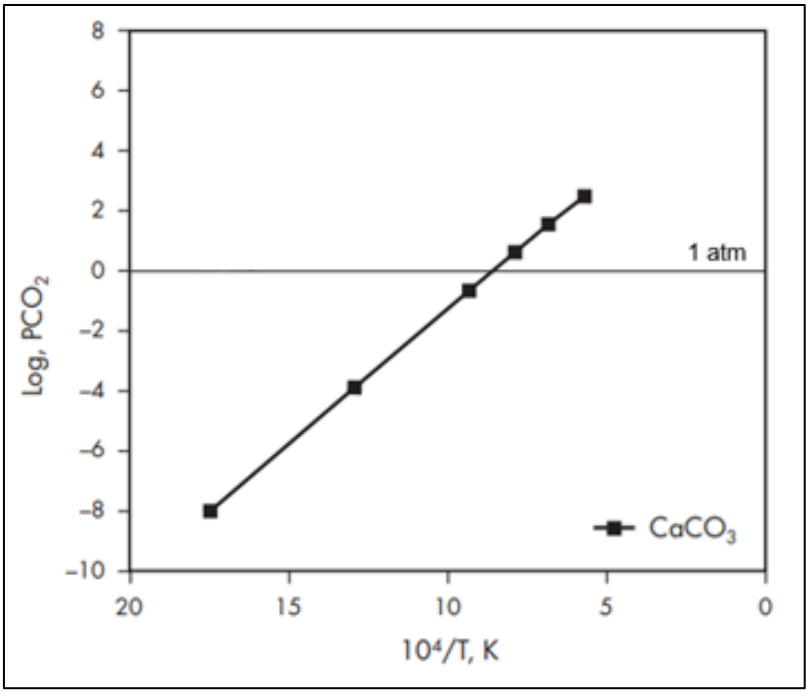

Figure 2.3 Decomposition equilibria of calcium carbonate (Chorney, 2019)

The shrinking core model could explain the calcination of calcium carbonate ($CaCO_3$) particles at high temperatures. As calcium carbonate decomposes, increasing temperatures are necessary to calcine further. With the effect of increasing temperature, an oxide layer (CaO) is formed, and the thermal conductivity of this oxide layer is lower than that of calcium carbonate, illustrated in Figure 2.4 (Chorney, 2019).

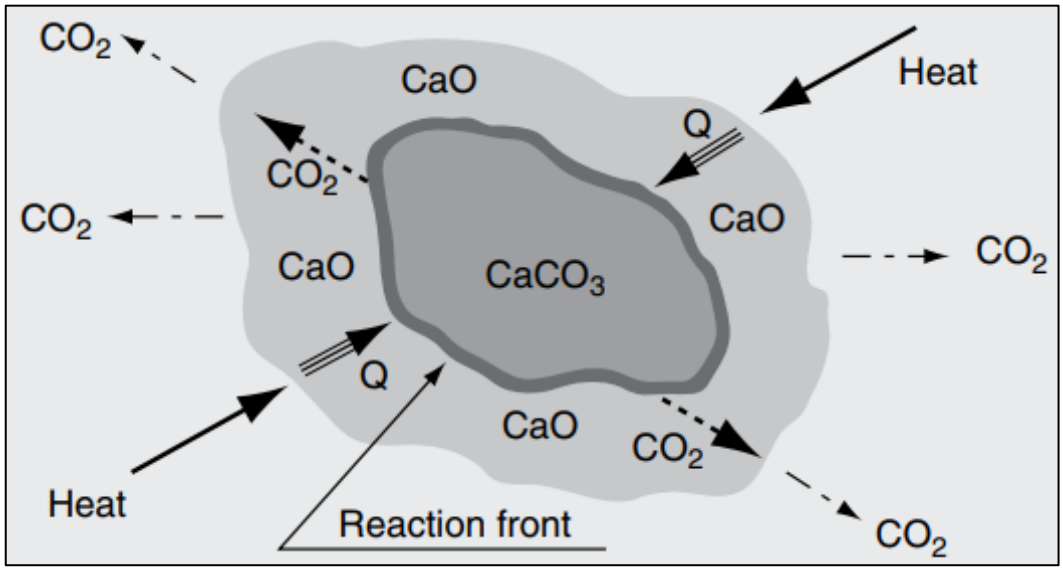

Figure 2.4 Calcination steps of calcium carbonate (Boateng, 2013)

Considering the decomposition temperature of calcium carbonate, the dissociation process of limestone particles is divided into five steps as follows (Boateng, 2013; Kumar et al., 2007):

(i) The heat is transferred from the surrounding atmosphere to the surface of the particle.

(ii) Heat is then transferred from the particle surface to the reaction front through a microstructure of the lime (CaO).

(iii) Heat arriving at the reaction front results in the dissociation of calcium carbonate ($CaCO_3$) into lime (CaO) and carbon dioxide (CO_2).

(iv) The carbon dioxide (CO_2) produced moves from the reaction front to the particle surface.

(v) The carbon dioxide (CO_2) moves away from the particle surface into the surrounding atmosphere.

There are several factors that affect the calcination of limestone. These factors are highly interrelated and summarized as follows (Boynton, 1980):

The characteristics of the limestone: The degree of decrepitation, type of crystallinity, and impurities affect the removal of CO_2 from stone during calcination. In preheating, the heat causes fractures and cracks in the limestones due to thermal expansion. These cracks produced by the depreciation of stone provide the space to escape the CO_2 gas and accelerate the decomposition of stone. The degree of this decrepitation is much more for largely crystallized limestones than fine-grained stones with the resistance to this expansion stress. On the contrary, CO_2 gas hardly penetrates the crystal lattice in coarse crystalline limestone since microstructures are dense, so the release of CO_2 gas slows down compared to finely crystalline limestone at calcination temperatures. Moreover, the quantity and type of impurities in the limestone adversely affect the quality of resulting lime by combining the silica and other impurities.

The particle size: The calcination of large particles is more difficult than small particles because there is a long distance to expel the CO_2 gas from the interior part of the large particle. The required heat and time in the furnace are greater than the calcination of small particles, as the calcination always starts from the surface of the particle and proceeds towards the interior parts of the particle.

The calcination temperature: The calcination temperature of limestones is generally between 900°C and 1000°C in PCC synthesis (Miller, 2013). However, it has to be done an experiment in order to determine the optimum calcination temperature of specific limestone. Furthermore, the heating rate, including preheating stage in calcination, has a favorable impact on the quicklime quality. In the preheating stage, limestone expands thermally, and this expansion results in an increase in limestone porosity which has also influence on the reactivity of lime.

The calcination time: To achieve complete calcination of limestone, calcination duration for the stone particles plays an important role. A certain time is needed for the heat transfer from the outer surface of the particle into the interior core to escape the CO_2 gas.

2.3.1.2 Hydration of Quicklime

By mixing varying amounts of water and quicklime, a solid-liquid reaction occurs in the hydration stage of lime, as displayed in Equation 2.2 (Teir et al., 2005).

$$CaO_{(s)} + H_2O_{(l)} \rightarrow Ca(OH)_{2(s)} + \text{Heat}, \qquad \Delta H_{(\text{at } 35^{\circ}C)} = -65.47 \text{ kJ/mol} \quad (2.2)$$

Calcium hydroxide as the product of the hydration reaction could be in the form of a dry, putty, slurry, milk of lime, or saturated aqueous solution. Generally, the term slaking is used in the case of wet hydrate formations. Milk of lime with a lime solid concentration ranging from 1 to 20% is used for industrial PCC production (Boynton, 1980; Jimoh et al., 2018; Oates, 1998).

When quicklime is mixed with water, quicklime exhibits a great affinity for moisture and absorbs it into its pores. A chain reaction occurs as a result of this natural hygroscopicity of quicklime. The heat of hydration is generated as the water enters the surface pores. It leads the lime particle to fracture, shatter, and finally disintegrate completely into microparticles, either as crystalline dust or a colloidal suspension, depending on how much water is added. Some water accompanying the reaction evaporates, and some are adsorbed and combined as a hydroxide molecule. The hydrate obtained as a result of this highly exothermic reaction is whiter than the lime from which it is produced (Boynton, 1980).

In the case of complete slaking of pure quicklime, the weight of the quicklime increases by adding the water. Theoretically, 56 grams of calcium oxide reacts with 18 grams of water to produce 74 grams of calcium hydroxide. In other words, the water content of slaked lime could be calculated as 24.3%. However, in practice, the theoretical amount of water is not sufficient to achieve complete slaking since some

water can evaporate due to the heat of slaking as well as the free water that is not chemically bonded and acts as a film surrounds the hydrated particle (Boynton, 1980).

The main factors influencing the slaked lime is listed as (Boynton, 1980; Oates, 1998):

The amount of water: By adding an excess amount of water to quicklime, an adverse reaction occurs in which the lime is drowned, and the slaking of lime is retarded and incompleted. On the contrary, adding an insufficient amount of water causes the burning of the quicklime due to the high-temperature generation in the slaking. The hydrated mass on the surface of the particle prevents water penetration, resulting in unslaked calcium oxides on the interior part of the particle.

The particle size of the quicklime: Fine particles with high reactivity are first dissolved and hydrated, producing primary nuclei. On the other hand, coarse particles with lower reactivity dissolve and hydrate more slowly and contribute to crystal growth.

The reactivity of the quicklime: As the highly reactive particles dissolve in water, they form numerous calcium hydroxide nuclei (primary), producing a high level of supersaturation. Less reactive particles dissolve more slowly and produce a lower degree of supersaturation. This largely results in crystal growth in primary nuclei.

The temperature of water: The rate of calcium oxide solution increases rapidly as the temperature rises. As a result, an increase in the temperature of the water used for slaking quicklime favors the primary nucleation of calcium hydroxide.

The rate of agitation: The agitation rate during the slaking process could be of two types: high agitation rate and relatively low agitation rate. High agitation rate increases solution rates and reduces agglomeration. On the other hand, the low agitation rate ensures adequate distribution of lime in water. This adequate dispersion helps the quicklime reduce the local overheating, which can cause the boiling of the lime.

2.3.1.3 Carbonation

Carbonation is the last stage of PCC production, as being the fast formation of calcium carbonate ($CaCO_3$) in water. The milk of lime obtained from the slaking process is reacted with carbon dioxide (CO_2) from the calcination process to precipitate calcium carbonate. This carbonation route could be considered an environmentally friendly process as carbon dioxide is re-used (Jimoh et al., 2018). The overall reaction is expressed in Equation 2.3 (Teir et al., 2005).

$$Ca(OH)_{2(s)} + CO_{2(g)} \rightarrow CaCO_{3(s)} + H_2O_{(l)}, \qquad \Delta H_{(at\ 45°C)} = -112.48\ kJ/mol \quad (2.3)$$

Precipitation of $CaCO_3$ is determined by supersaturation which is affected by the product of the ionic concentrations of Ca^{2+} and carbonate ions in the aqueous solution. Four stages are involved in the precipitation of calcium carbonate (Domingo et al., 2006):

(i) Dissolution of $Ca(OH)_2$

In an aqueous solution, $Ca(OH)_2$ is very slightly soluble (Eq. 2.4 and Eq. 2.5). The dissolution of $Ca(OH)_2$ particles could be divided into two steps. These particles dissolve on the solid surface initially, and Ca^{2+} ions diffuse away from the solid surface to bulk solution, subsequently.

$$Ca(OH)_2 \leftrightarrow Ca^{2+} + 2OH^-(\text{solid surface}), \qquad K_{sp(at\ 25°C)} = 10^{-5.3} \quad (2.4)$$

$$Ca^{2+} + 2OH^-(\text{solid surface}) \leftrightarrow Ca^{2+} + 2OH^-\ (\text{bulk solution}) \quad (2.5)$$

(ii) Formation of carbonate ions by mass transfer between CO_2 and water phases

In this stage, gaseous CO_2 dissolves in water; then it forms aqueous CO_2 or carbonic acid (H_2CO_3) for the most part (Eq. 2.6). H_2CO_3 formed as a result of adsorption of CO_2 by water dissociates into bicarbonate (HCO_3^-) ion and carbonate ion (CO_3^{2-}) (Eq. 2.7 and Eq. 2.8). Although these reactions are rapid, only around 1% of the CO_2 absorbed in water is transformed into carbonate ions.

$CO_{2(g)} + H_2O \leftrightarrow CO_{2(aq)}$ or H_2CO_3, $K_{(at\ 25°C)}=10^{-1.5}$ (2.6)

$H_2CO_3 \leftrightarrow HCO_3^- + H^+$, $K_{(at\ 25°C)}=10^{-6.3}$ (2.7)

$HCO_3^- \leftrightarrow CO_3^{2-} + H^+$, $K_{(at\ 25°C)}=10^{-10.3}$ (2.8)

(iii) Precipitation reaction

When Ca^{2+} ions react with CO_3^{2-} in the aqueous solution, the calcium carbonate forms. At high concentrations of reactants, the precipitation reaction results in an amorphous phase of calcium carbonate which has spherical shapes less than 1 µm diameter. Since the amorphous phase has a higher solubility than the crystalline phase, the amorphous phase tends to transform into the more stable crystalline phase (Eq. 2.9 and Eq. 2.10).

$Ca^{2+} + CO_3^{2-} \leftrightarrow CaCO_{3(amorphous)}$, $K_{sp(at\ 25°C)}=10^{-8.3}$ (2.9)

$Ca^{2+} + CO_3^{2-} \leftrightarrow CaCO_{3(calcite)}$, $K_{sp(at\ 25°C)}=10^{-8.3}$ (2.10)

(iv) Crystal growth

Supersaturation has the primary impact on particle size, although excess species that could also behave as additives also have an impact on final crystal habit. Inducing varied growth rates on crystal faces could result in a modification in particle morphology. The morphology of the growing crystal is restricted by the faces with the slowest growth rate (Mullin, 1997). The nonpolar {104} face contains equimolar amounts of calcium and carbonate ions in calcite crystals. The scalenohedral morphology of calcite crystal is obtained under the condition that the relative growth rate of the {104} face is high enough to cause disappearance. The growth of the crystal face results in the formation of neutral $CaCO_3$ in the crystal-solution interphase. On the surface of the crystal, Ca^{2+} and CO_3^{2-} ions exhibit different adsorption behavior (Brown et al., 1993). Therefore, the morphology of $CaCO_3$ is influenced by the Ca^{2+} and CO_3^{2-} ions in the bulk solutions. Under the interaction of Ca^{2+} and CO_3^{2-} ions stoichiometrically, rhombohedral calcite crystals form. In the presence of excess Ca^{2+} ions, the morphology of $CaCO_3$ crystals is scalenohedral.

2.3.2 Precipitated Calcium Carbonate (PCC) Applications

Precipitated calcium carbonate is produced to meet the high global demand in various fields of industry: paper, paint, adhesive, plastic, sealants, etc. It is possible to produce PCCs with various morphology, particle size, chemical purity and, surface area depending on the industrial needs. In 2013, the estimated global consumption of PCC is shown in Figure 2.5. It is seen that the paper industry is one of the leading industries promoting PCC production worldwide as well as paint, plastic, and sealant (Jimoh et al., 2018; Domingo et al., 2006).

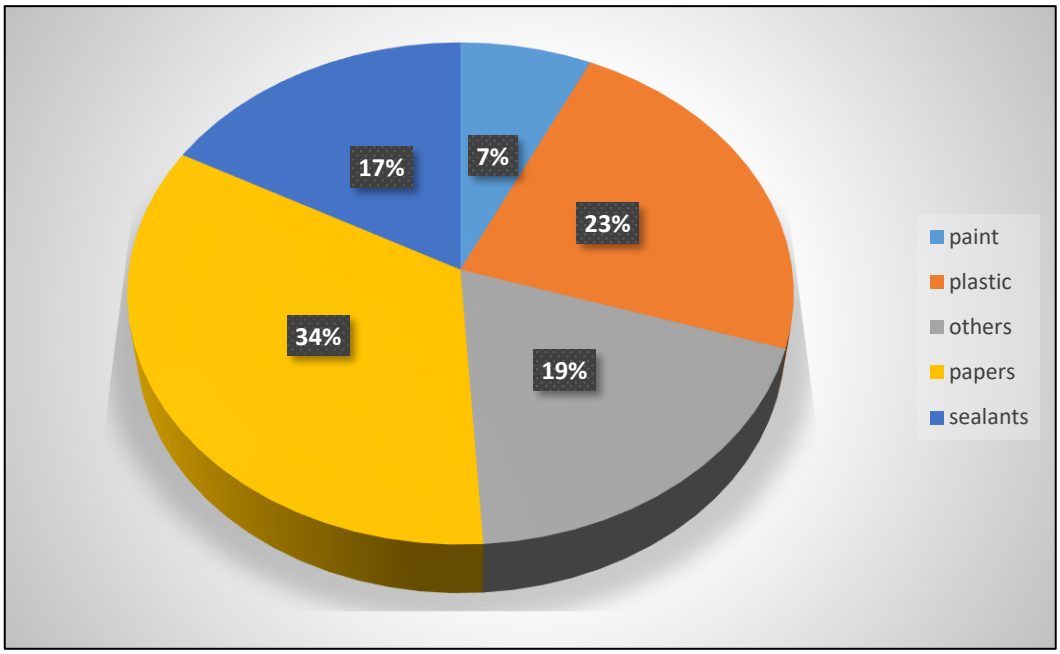

Figure 2.5 The estimated global consumption of PCC in 2013 (Jimoh et al., 2018)

PCC is used in the paper industry as an alternative filler instead of fillers such as talc, kaolin, titanium oxides, and ground calcium carbonate. The addition of PCC as a filler to papers has several benefits. It provides the production of high quality papers in terms of optical, durability, smoothness, and ink adsorption properties. It also reduces costs in paper production due to its low cost, particularly when used instead of titanium oxide (TiO_2). Moreover, the addition of PCC filler does not cause abrasion and dusting under certain production conditions (Jimoh et al., 2018). The

chemical additives in papermaking, paper smoothness, and printing characteristics are affected by the particle size distribution and shape of the PCC crystals (Teir et al., 2005).

In the plastic industry, PCC is extensively used as a filler for the purposes of partial substitution of the costly polymers, reducing costs and improving impact resistance associated with higher elastic modulus, and thermal conductivity (Jimoh et al., 2018).

Precipitated calcium carbonate fillers are also used in the paint industry as a low-price extender to improve brightness and weather resistance of paints. In addition, they are used in various paint formulations combined with micronized talc or calcined clay to reduce expensive titanium oxide (TiO_2) consumption. Generally, PCCs with a size of 5-14 µm are used in flat and semi-gloss paints. In addition, PCCs with an ultrafine size of 1-5 µm could be used on glossy finishes to reduce paint sagging and adjust consistency (Jimoh et al., 2018).

PCC fillers are utilized in adhesive and sealant composites manufacturing. Cost reduction, rheology modification, and strengthening are the main purposes for the utilization of PCC fillers (Jimoh et al., 2018). PCCs with a coarse size range of 30-45 µm are used in the paste, whereas the PCCs with a fine size range of 1-15 µm are used in adhesive and sealants (Said et al., 2013).

PCCs with 93% and higher brightness values (measured relative to $BaSO_4$) are used as an effective filler (Jimoh et al., 2018). Generally, rhombohedral PCCs providing a high specific surface area are used in plastic and sealant industries. On the other hand, scalenohedral PCCs are applied in the paper and paint industries (Ukrainczyk et al., 2007).

In addition to the these applications, PCC is used in toothpaste and powder as a mildly abrasive substance and filler. PCC coated with fatty acids is also utilized in printing ink formulations. Since calcium carbonate decomposes into carbon dioxide and quicklime, PCC also performs as a flame retardant (Oates, 1998).

CHAPTER 3

MATERIALS AND METHODS

3.1 Materials

In this study, marble waste and limestone were used as raw materials in the comparison experiments for the production of precipitated calcium carbonate. Marble wastes were collected from different faces of a quarry located in the Muğla-Yatağan region of Turkey. Limestone samples that have already been used in the precipitated calcium carbonate production were taken from Afyonkarahisar.

Marble waste and limestone samples were first crushed by jaw crusher followed by roll crusher to achieve the desired sizes. Crushed samples were sieved to size ranges used in the calcination process and stored in sealed plastic bags to prevent the absorption of moisture from the atmosphere.

3.1.1 Mineralogical Analyses of Samples

Mineralogical analyses of the marble and limestone samples were carried out by the X-Ray Powder Diffraction technique (XRD) using the Rigaku Ultima IV diffractometer. During the analyses, data were recorded from 5° to 80° (2θ). The XRD analysis of the marble sample is shown in Figure 3.1. According to the XRD patterns and peak intensities of minerals, calcite is the major carbonate composition of the marble sample. The small amounts of dolomite and aragonite are the minor carbonate minerals in the sample. Low intensities of quartz and hematite minerals are also detected in the XRD pattern, and they are regarded as the main impurities in the marble sample. For the limestone sample, the XRD analysis is shown in Figure 3.2. The minerals identified in the XRD pattern of limestone are similar to marble waste.

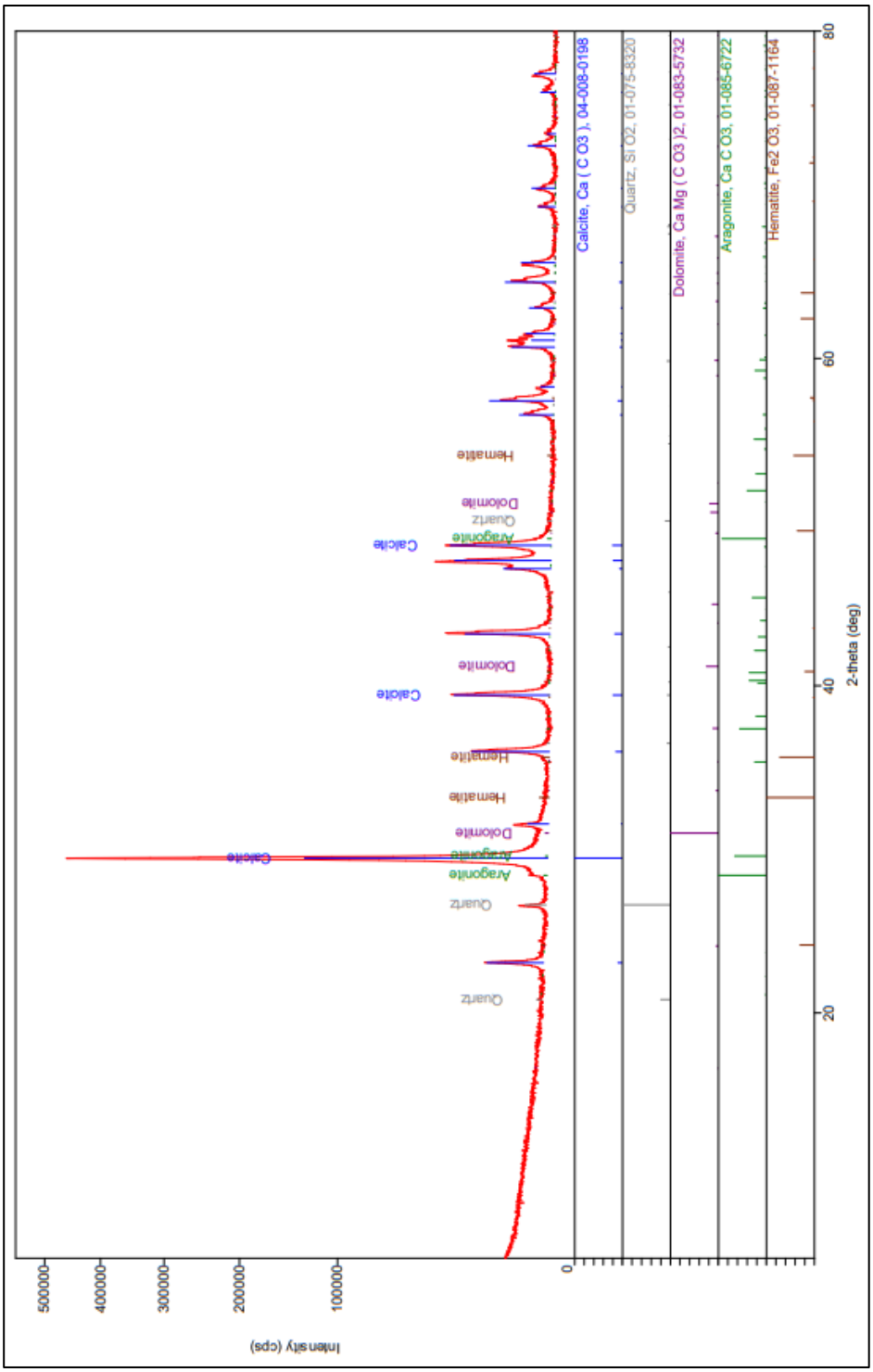

Figure 3.1 The XRD pattern of the marble waste

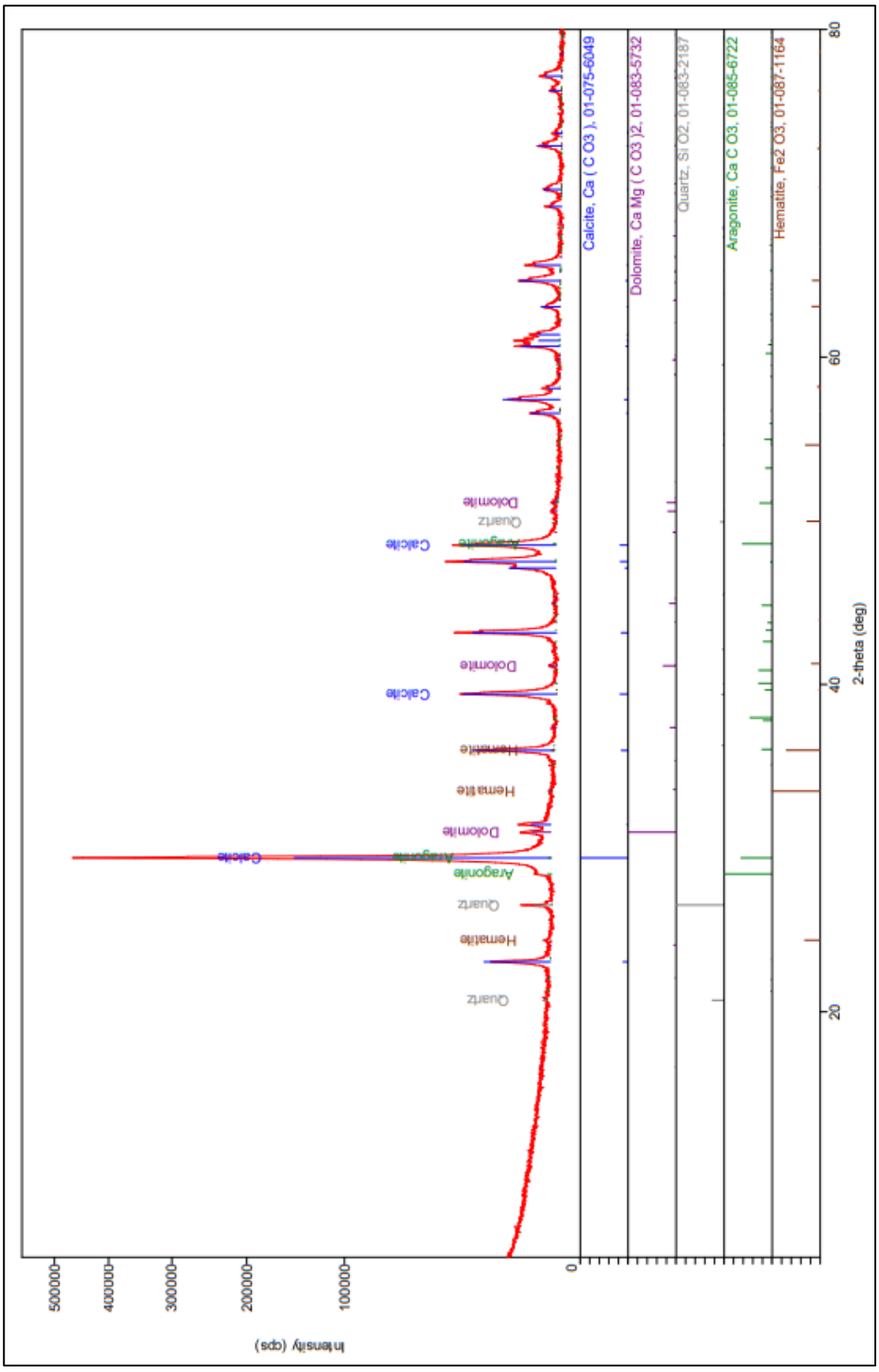

Figure 3.2 The XRD pattern of the limestone

3.1.2 Chemical Analyses of Samples

Chemical composition of marble waste and limestone samples determined by X-Ray Fluorescence Spectrometer (XRF) are given in Table 3.1. According to results, it is observed that the marble waste and limestone are of high purity with 55.21% and 55.48% calcium oxide (CaO) composition, respectively. Small amount of magnesium oxide (MgO), iron oxide (Fe_2O_3), silicon oxide (SiO_2) and aluminum oxide (Al_2O_3) is present in both samples. Loss on ignition (LOI) of marble waste (43.56 %) and limestone (43.53%) is nearly the same.

Table 3.1 Chemical analysis of marble waste and limestone

Constituents	**Marble Waste (wt.%)**	**Limestone (wt.%)**
CaO	55.21	55.48
MgO	0.71	0.70
Fe_2O_3	0.16	0.21
SiO_2	<0.1	<0.1
Al_2O_3	<0.1	<0.1
LOI	43.56	43.53

3.1.3 Thermal Analyses of Samples

The thermal characterization of marble waste and limestone was determined using Thermogravimetric Analysis (TGA) and Differential Scanning Calorimeter (DSC) analysis methods. Perkin Elmer Simultaneous Thermal Analyzer (STA) 6000 instrument was used to record sample mass as a function of temperature as the temperature is increased for TGA analysis and, to measure the difference in the heat flow between the reference material and sample for DSC analysis. The samples were heated from 30°C to 950°C at the heating of 10°C/min in an inert atmosphere (nitrogen flow).

From the TG profile of marble waste, it is observed that marble waste decomposes approximately between the temperatures of 600°C to 900°C. This decomposition resulting from the loss of carbon dioxide corresponds to a portion of 43.464% of the weight. The temperature with the highest weight change rate is shown as 830.26°C. According to the DSC profile of marble waste, the ΔH value of this endothermic decomposition reaction of marble waste was calculated as 2449.04 J/g, based on the area under the curve of which the onset and end temperature values are 692.53°C and 868.35°C, respectively.

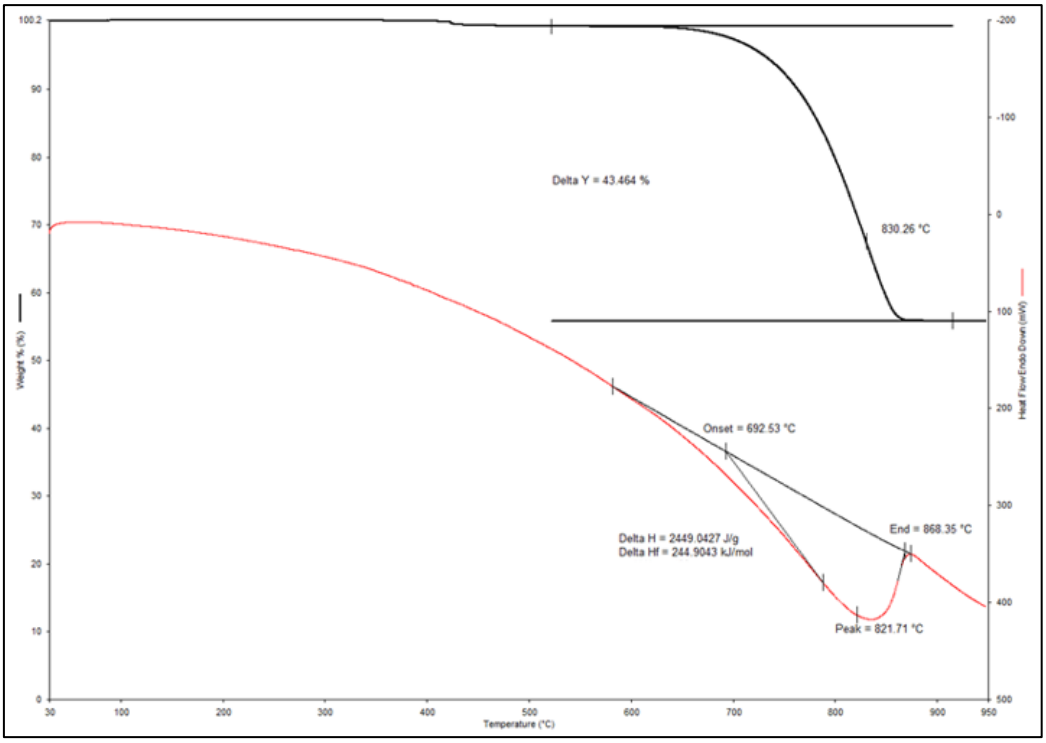

Figure 3.3 TG-DSC profile of the marble waste

It could be seen from the TG profile of limestone that the sample decomposes at temperatures ranging from 600°C to 900°C. The decomposition caused by the loss of carbon dioxide corresponds to 43.492% of the total weight. The temperature with the highest rate of weight change takes place at 835.13°C. The ΔH value of this endothermic reaction of limestone was determined as 1999.7213 J/g using the DSC profile of limestone, based on the area under the curve with onset and end temperature values of 698.96°C and 865.54°C, respectively.

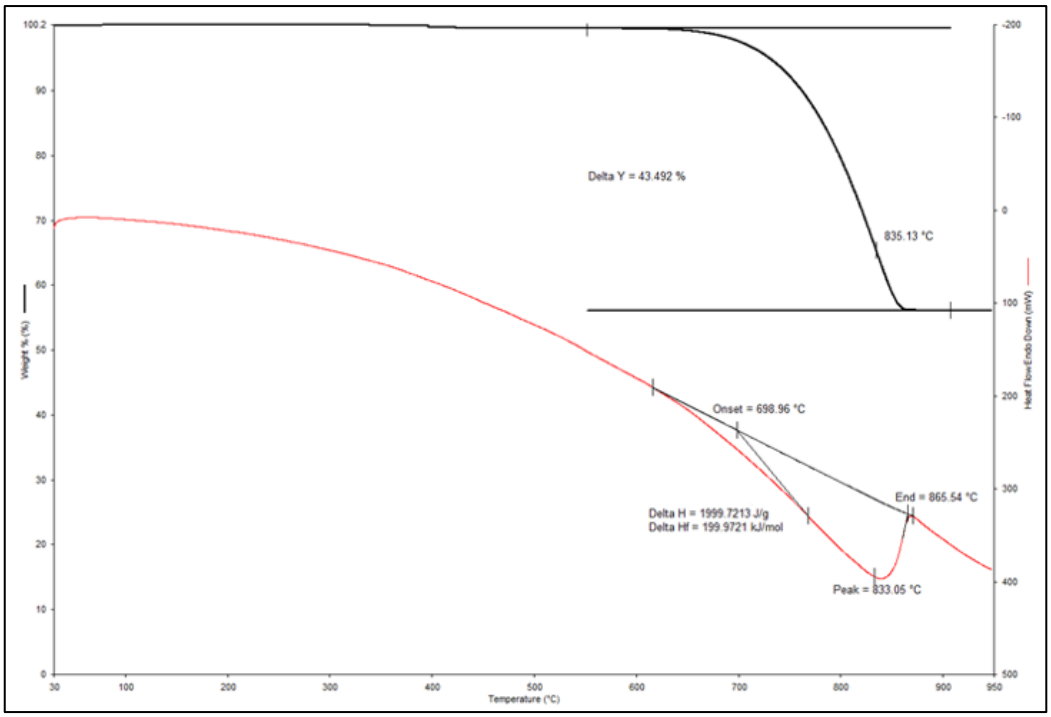

Figure 3.4 TG-DSC profile of the limestone

3.2 Methods

3.2.1 Calcination Experiments

Calcination experiments were carried out comparatively for limestone and marble wastes after necessary comminution stages. The effects of variable temperature, duration, and particle size range parameters on calcination efficiency were investigated during experiments (Table 3.2).

Table 3.2 The calcination parameters and their levels

Parameters	Levels
Calcination Temperature (˚C)	900, 950, 1000
Calcination Time (min.)	10, 20, 30, 60, 90, 120
Particle Size Ranges (mm)	-12.7+6.35, -25.4+12.7

The experiments were carried out in a muffle furnace using flat alumina crucibles of 60 mm-60 mm square dimensions. The sample amount varied between 50-60 grams for each experiment. After the samples placed in the muffle furnace reached the desired temperature from room temperature, the calcination duration was examined. In this way, a more realistic calcination environment has been tried to be created by imitating the preheating zone in industrial furnaces. The muffle furnace reached the desired temperature with an average heating rate of 15˚C/min. At the end of the process, the samples which were subjected to elevated temperatures were removed from the furnace and cooled to constant mass in the desiccator to determine calcination efficiencies calculating its weight loss.

For the industrial production of calcium oxide in typical kilns, in general, the acceptable size range of feed stone ranges from a minimum of 20 mm to a top size of 175 mm (Oates, 1998). However, particle size ranges used in the calcination experiments were limited by the muffle furnace and crucible dimensions. Therefore, the suitable top size of the particles for furnace and crucible dimensions was chosen as 25.4 mm.

Although the dissociation temperature of calcite is around 900°C at 1 atm in the CO_2 atmosphere, the calcination temperature of a particular calcite stone can varies depending on the characteristic of stone such as decrepitation tendency, crystallinity, and operational parameters such as CO_2 pressure, and the temperature which are discussed in Section 2.3.1.1. In practice, higher temperatures than the theoretical value are required generally to decompose the stone up to its core, completely, for a certain duration (Boynton, 1980). For this reason, experiments were carried out at temperatures of 900°C and higher.

3.2.2 Hydration of Lime Experiments

In hydration experiments, the limes of two different origins were reacted with distilled water at ambient temperature (about 25°C) in a 250 ml beaker using a

vertical agitator at a constant stirring rate of 60 rpm. Three different limes to water ratios (1:3.5, 1:4.0, and 1:4.5) were investigated by mixing lime with water (Table 3.3). The quicklime of marble and limestone origin were fed uniformly and slowly into the beaker containing distilled water and stirring at 60 rpm. The thermometer was used to detect the increase in temperature over time during the reaction.

Table 3.3 The hydration of lime parameters and their levels

Parameters	**Levels**
Particle size interval of lime feed	-19.5+12.7 mm
Lime to water ratio (by weight)	1:3.5, 1:4.0, 1:4.5
Lime weight (g)	30
Stirring rate (rpm)	60

The hydration experiments were carried out using quicklime of marble and limestone origin obtained under optimum calcination conditions. Although the particle size range was -25.4+12.7 mm for optimum conditions, a narrow particle size range of -19.5+12.7 mm was chosen to eliminate the effect of particle size and provide uniformity of hydration experiments. Additionally, the size range of quicklime is up to 20 mm for modern batch slakers (Oates, 1998).

In the experiments, distilled water was used since some species such as carbonates, sulfites, and sulfates in the water have an adverse effect on the slaking process. The slaking with municipal water, which contains these species, results in less primary nucleation and increased crystal growth compared to slaking with distilled water (Oates, 1998).

The properties of the slaked lime are mainly dependent on the initial conditions of the reaction and the reactivity of quicklime. Slaked limes with acceptable fine particles are produced by reactive quicklime mixing in a limited volume of water with a sufficient stirring rate. Reactive quicklime causes more primary nucleation than less reactive quicklimes, resulting in a proportion of particles around less than

1 μm. In this respect, it is essential to understand whether there is a difference between marble and limestone. The sufficient agitation rate also plays an important role in eliminating localized dead spots of quicklime, dispersing lime particles in suspension, and accelerating rates of slaking (Oates, 1998).

Moreover, the lime slaking processes are extremely exothermic, as adding calcium oxide to water generates a lot of heat, resulting in a significant temperature increase. One of the key elements to optimizing the slaking reaction is controlling this temperature variation. For this purpose, it has been investigated whether industrially desired temperature ranges are provided according to the temperature profiles resulting from the exothermic reaction at the recommended lime to water ratios. Lime to water ratios in the range of 1:3.0 and 1:4.5 are recommended to avoid burning and/or drowning the lime particles. The slaking temperature is trying to keep in the range generally 85 to 95°C for batch slaking, 80 to 85°C for continuous slaking while adding the lime to water (Boynton, 1980; Oates, 1998).

As the temperature of the hydrated lime slurry starts to reduce, dilution water was added to make the desired concentration of milk of lime for the carbonation process. The milk of lime was agitated at a rate of 60 rpm for 30 minutes for the production of well dispersed and finely divided particles of calcium hydroxide in a suspension. Prepared milk of lime suspension was screened at 75 μm to remove coarse unreacted lime particles present as grit in the hydrate and impurities present in the stone.

3.2.3 Carbonation Experiments

The lab scale autoclave shown in Figure 3.5 was used in carbonation experiments of milk of lime to provide high CO_2 pressures. The autoclave was preferred to yield a greater overall reaction rate due to the high solubility of CO_2 under elevated pressures. CO_2 pressure values of 5-10 bar could be used for precipitated calcium carbonate production. (Teir et al., 2005). Therefore, experiments were carried out under constant CO_2 pressure values of 5 and 10 bar at ambient temperature.

300 ml of prepared milk of limes of marble and limestone origins with 5% and 10% concentrations were placed into autoclave which contains a Teflon cylinder with 1 liter capacity. Experiments were carried out by connecting the required CO_2 gas cylinder to the autoclave and stirring the suspension with the help of a Teflon mixing impeller under constant pressure. The temperature was monitored with a thermometer inside the autoclave during the experiment.

Figure 3.5 The lab-scale autoclave used in the carbonation experiments

Typically, the solid mass concentration of $Ca(OH)_2$ slurry could be about 20% for the PCC production (Jimoh et al., 2018). Due to the high viscosity of the suspensions at ambient temperatures, the lower concentrations of $Ca(OH)_2$ (5% and 10%) were chosen for the precipitation experiments in the lab-scale autoclave.

During the precipitation of calcium carbonate reaction, the milk of lime suspension was continuously agitated under a high shear rate of 750 rpm (Souto et al., 2008). The agitation has a significant effect on the formation of crystal growth. Under the

high agitation, the precipitation rate increases due to high particle-particle collision and attrition of precipitated calcium carbonates. In addition, the formation of clusters or groups of precipitates is prevented at high agitation rates. (Afridi et al., 2008).

The parameters used in the experiments are listed in Table 3.4.

Table 3.4 The carbonation of milk of limes parameters and their levels

Parameters	**Levels**
Solid mass concentration of $Ca(OH)_2$(%)	5, 10
CO_2 Pressure (bar)	5, 10
Stirring rate (rpm)	750

In order to determine whether the reaction was complete, pH values and a decrease in temperature were controlled during the reaction. The pH value of milk of lime slurry, which is 12 or higher at the beginning of the experiment, decreases to 8±1 after the complete precipitation of calcium carbonate. At the beginning of the precipitation reaction, the pH of the slurry remains alkaline due to the suspended $Ca(OH)_2$ particles which dissociates to Ca^{2+} ions. As the reaction proceeds, the concentration of $Ca(OH)_2$ decreases, while the concentration of H^+ ions due to the continuous dissolution of CO_2 in the suspension increases and the pH value of the suspension reaches almost neutral value. The decrease in pH value of the solution indicates the complete carbonation of $Ca(OH)_2$ (Souto et al., 2008).

In addition to the pH value of the reaction, the decrease in temperature from its highest value indicates the reaction is over. The produced PCC at the end of the carbonation process was filtrated and then dried at 105°C for 3 hours in an oven.

For the analysis of the particle size distribution of the PCC product, Malvern Mastersizer 2000 equipment were used. The color of PCCs was analyzed with Luci 100 (Dr. Lange Co.) which is the spectral color measurement equipment. The whiteness and yellowness indexes of PCC produced from marble waste and

limestone were calculated according to ASTM method E313, using CIE XYZ color space results of samples obtained from Luci 100. The values of these color spaces were measured relative to $BaSO_4$ as reference material.

In order to determine the crystal morphology of PCCs, the scanning electron microscopy (SEM) analyses were carried out in the Materials and Metallurgical Engineering Department at METU.

The flowchart of production of PCC is illustrated in Figure 3.6.

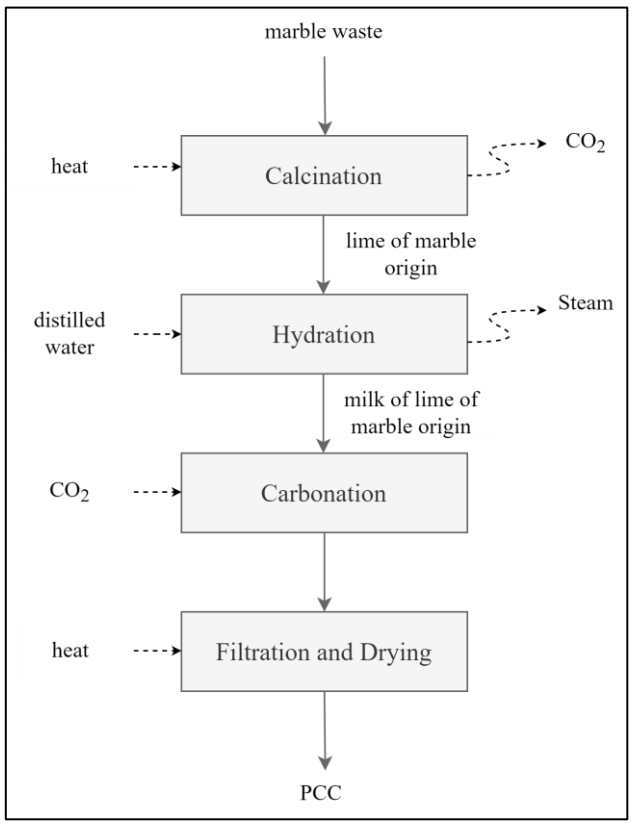

Figure 3.6 Flowchart of PCC production by carbonation route

CHAPTER 4

RESULTS AND DISCUSSION

4.1 Calcination Experiments

As the first stage of production of PCC, samples were calcined in the muffle furnace. The calcination efficiencies of marble waste and limestone are given in Table A.1 and Table A.2, respectively. These efficiencies are based on the total weight loss in the samples during the calcination due to the loss of CO_2 content. Weight loss due to the small amount of impurities and organic matter that exists in the stones was ignored. The calcination efficiencies were calculated according to Equation 2.10.

$$\text{Efficiency (\%)} = \left(\frac{\text{Total weight loss}}{\text{Sample weight before calcination} * 0.44}\right) * 100 \qquad (2.10)$$

Theoretically, the maximum loss in weight occurs in the case of 44% of the CO_2 content being released for pure calcium carbonate. However, in practice, it is not possible the removal of 100% of the in the stone because of the slight surface adsorption of CO_2 (Boynton, 1980).

Experiments were carried out using limestone and marble wastes samples to determine whether there is a significant difference in calcination efficiencies between samples and optimization of the calcination process. At 900, 950, and at 1000˚C, a comparison of the calcination efficiencies of marble waste and limestone in both particle size intervals (-12.7+6.35 and -25.4+12.7 mm) over time (10, 20, 30, 60, 90, and 120 min.) is shown in Figure 4.1, Figure 4.2, and Figure 4.3. According to these figures, it is not observed any significant difference between the calcination efficiencies of marble waste and limestone under the examined parameters and their levels. Small differences are thought to be due to the characteristics and nature of the stones, as mentioned in Section 2.3.1.1.

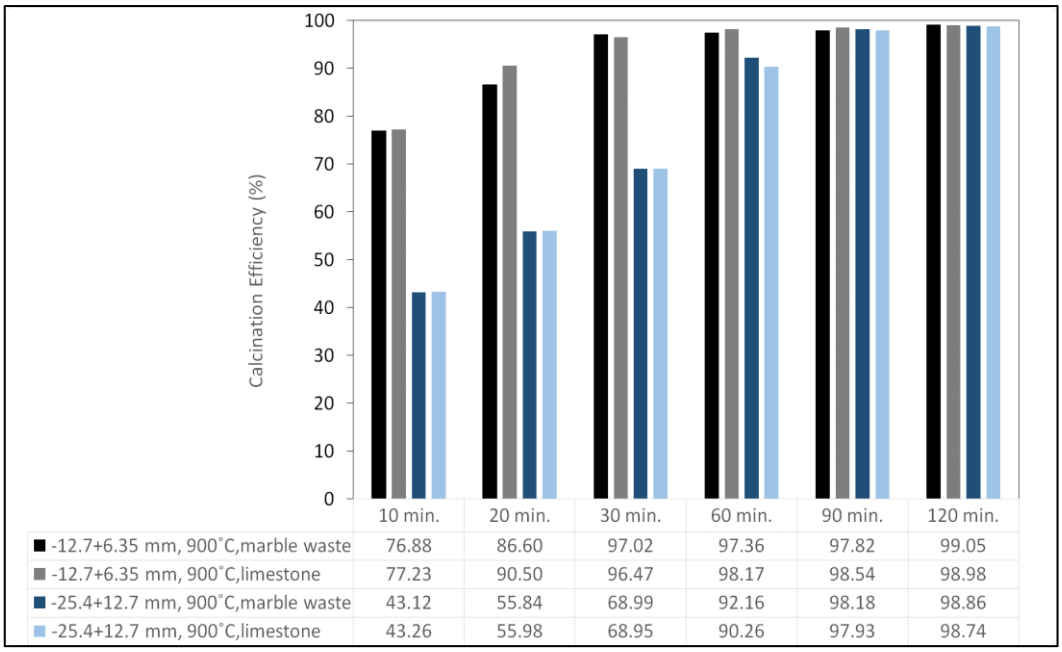

	10 min.	20 min.	30 min.	60 min.	90 min.	120 min.
-12.7+6.35 mm, 900˚C,marble waste	76.88	86.60	97.02	97.36	97.82	99.05
-12.7+6.35 mm, 900˚C,limestone	77.23	90.50	96.47	98.17	98.54	98.98
-25.4+12.7 mm, 900˚C,marble waste	43.12	55.84	68.99	92.16	98.18	98.86
-25.4+12.7 mm, 900˚C,limestone	43.26	55.98	68.95	90.26	97.93	98.74

Figure 4.1 The calcination efficiencies of marble waste and limestone at 900˚C for the size intervals of -12.7+6.35 and -25.4+12.7 mm

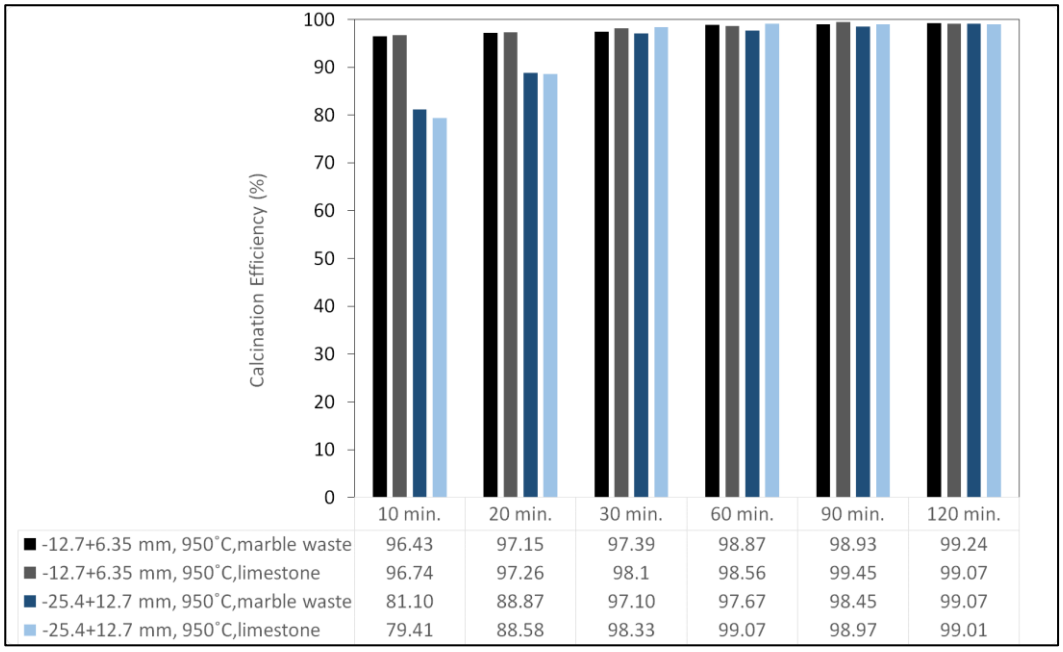

	10 min.	20 min.	30 min.	60 min.	90 min.	120 min.
-12.7+6.35 mm, 950˚C,marble waste	96.43	97.15	97.39	98.87	98.93	99.24
-12.7+6.35 mm, 950˚C,limestone	96.74	97.26	98.1	98.56	99.45	99.07
-25.4+12.7 mm, 950˚C,marble waste	81.10	88.87	97.10	97.67	98.45	99.07
-25.4+12.7 mm, 950˚C,limestone	79.41	88.58	98.33	99.07	98.97	99.01

Figure 4.2 The calcination efficiencies of marble waste and limestone at 950˚C for the size intervals of -12.7+6.35 and -25.4+12.7 mm

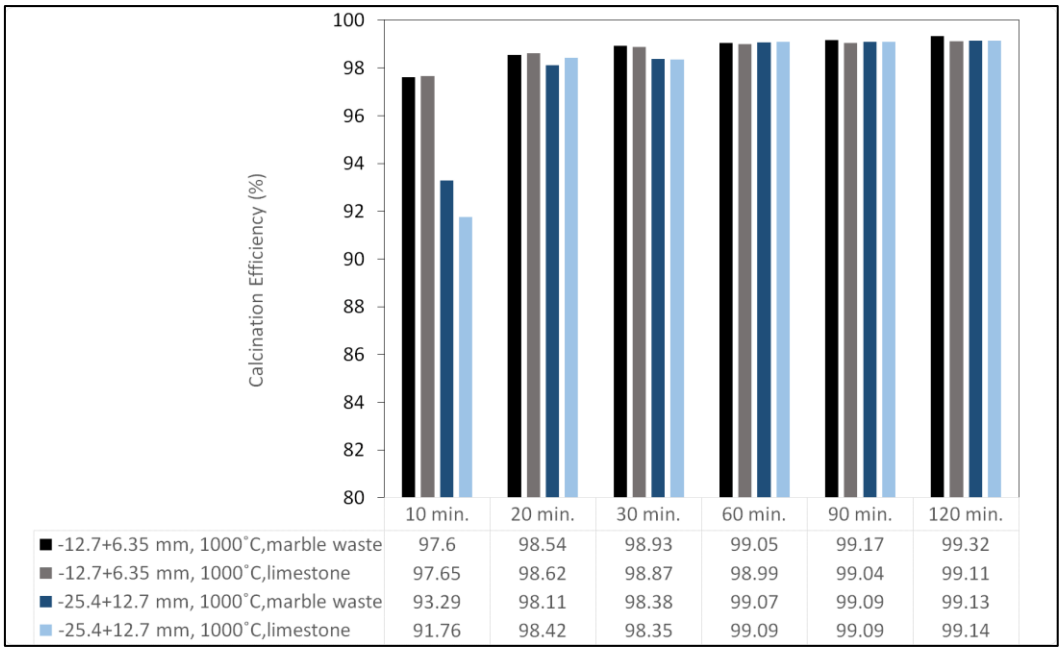

Figure 4.3 The calcination efficiencies of marble waste and limestone at 1000˚C for the size intervals of -12.7+6.35 and -25.4+12.7 mm

The effects of calcination temperatures (900, 950, and 1000˚C), particle size intervals (-12.7+6.35 and -25.4+12.7 mm), and calcination duration (10, 20, 30, 60, 90, and 120 min.) as three main factors affecting the calcination characteristics of samples, were investigated to determine the optimum calcination conditions of marble waste sample.

4.1.1 Effect of Temperature on the Calcination of Marble Waste

The calcination efficiency of marble waste with the particle size of -25.4+12.7 mm is shown in Figure 4.4 at varying temperature values. It is clearly seen that these efficiencies reach the highest value at 1000˚C. Particularly, in short calcination duration such as 10, 20, and 30 min., a significant difference is observed between the efficiencies at 900 and 1000˚C. For a calcination time of 10 min., the calcination efficiency (43%) at 900˚C is almost half the efficiency (93%) at 1000˚C. As shown in Figure 4.5, it is observed that this difference decreases when the particle size of

the marble waste reduces to -12.7+6.35 mm. As a result of the calcination duration of 10 minutes, the calcination efficiency at 900˚C is 77%, while it is 98% at 1000˚C.

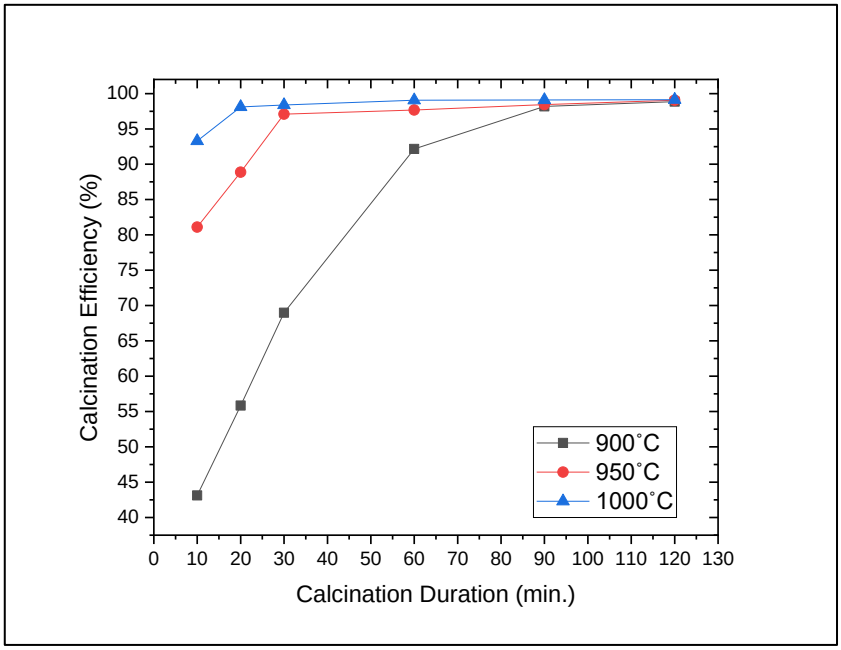

Figure 4.4 The calcination efficiencies of marble waste with a particle size interval of -25.4+12.7 mm in varying calcination temperatures

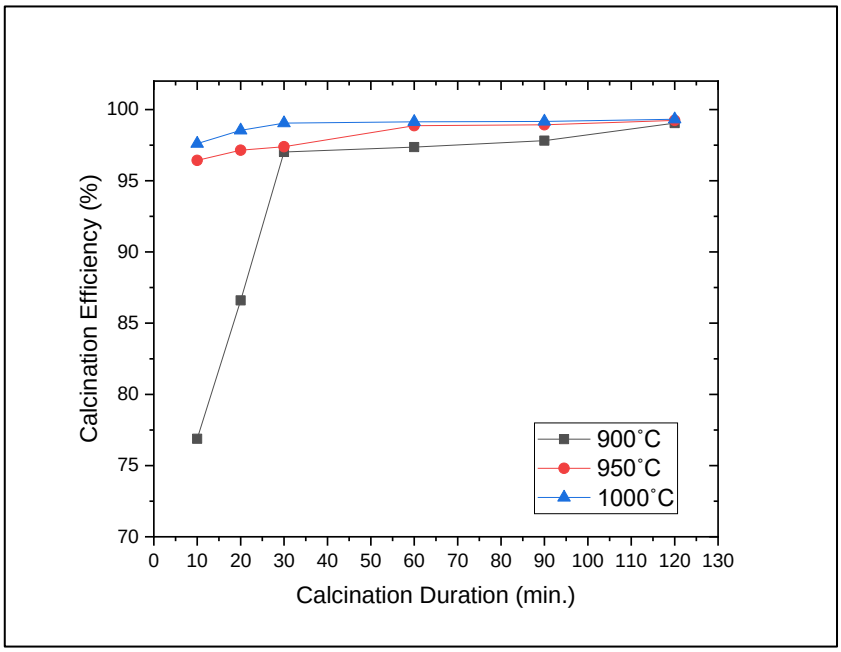

Figure 4.5 The calcination efficiencies of marble waste with a particle size interval of -12.7+6.35 mm in varying calcination temperatures

According to Figure 4.4 and Figure 4.5, 1000˚C could be considered the optimum temperature for calcination of marble waste since the calcination efficiency of marble wastes at 1000˚C is the highest in both particle size ranges.

4.1.2 Effect of Time on the Calcination of Marble Waste

The calcination efficiencies are given in Figure 4.6 in varying retention times for studied particle size interval at 1000˚C, which was chosen as optimum calcination temperature in Section 4.1.1.

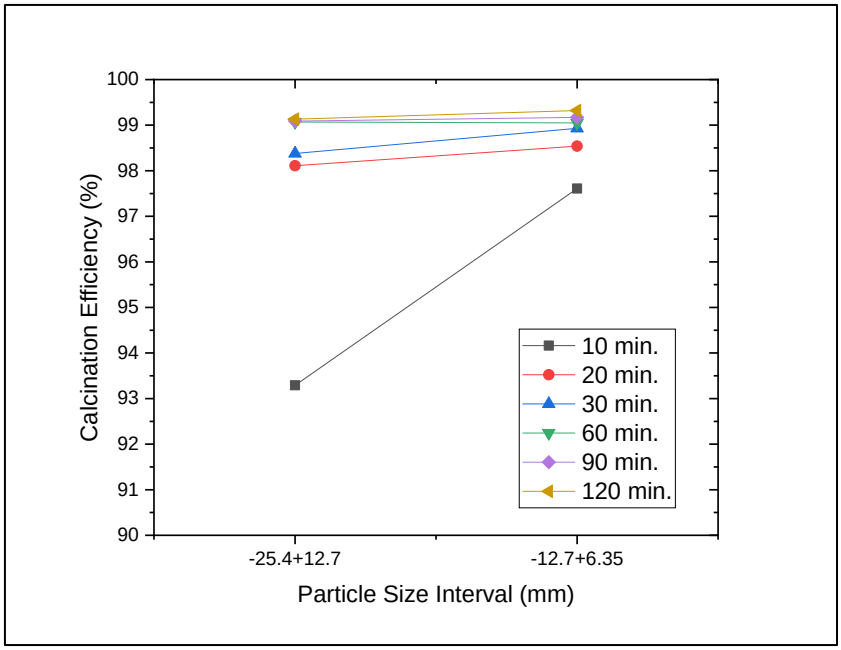

Figure 4.6 The calcination efficiencies of marble waste at 1000˚C in varying particle size ranges

It is necessary to maintain heat at a constant temperature for a certain time in order to be completely calcined the stones. Therefore, short or long residence times affect the calcination efficiency. Insufficient time results in the presence of uncalcined calcium carbonate in the center of the particle. On the contrary, prolongation of calcination time at higher temperatures causes the formation of an impervious surface by closing the pores on the surface of the particle. In this case, the lime formed is called hard-burned lime with lower reactivity compared to high calcium

lime. Additionally, as the retention time of particles in the furnace increases, the rate of production decreases, and the production costs increase (Boynton, 1980; Muslim et al., 2015).

According to Figure 4.6, the desired efficiency could not be reached for both size ranges in 10 minutes. However, it is obvious that 20 minutes is sufficient for efficiency to be higher than 98%, and there is no significant increase in efficiency after 20 minutes for both size ranges. Besides, a longer calcination time will be extra costly and can result in the formation of hard burned lime.

4.1.3 Effect of Particle Size on the Calcination of Marble Waste

The calcination efficiencies for particle size ranges of -25.4+12.7 and -12.7+6.35 mm are shown in Figure 4.7 in varying calcination temperatures during 20 min. calcination time. The effect of the lower calcination temperatures on particle size ranges is also seen in Figure 4.7 during the 20 minutes calcination duration.

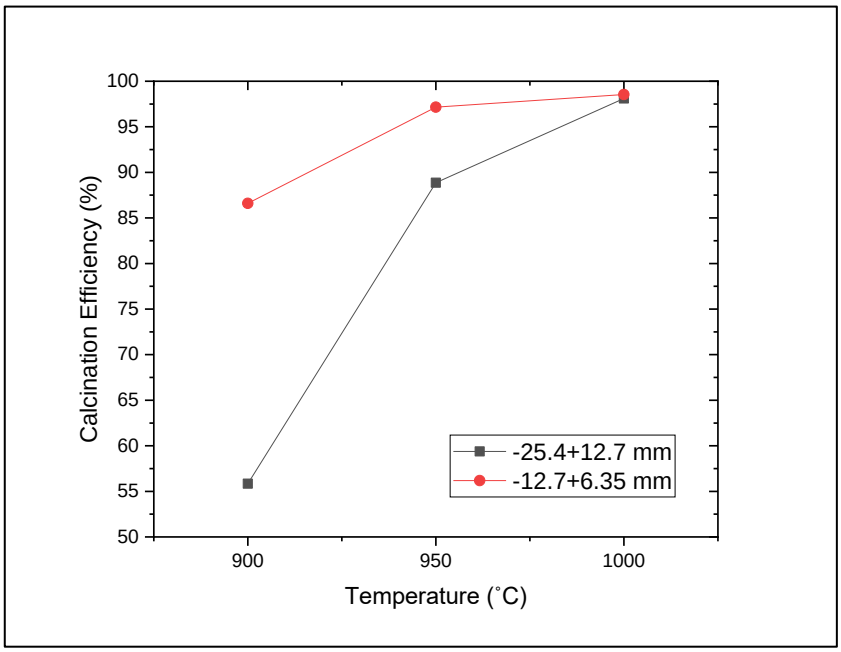

Figure 4.7 The calcination efficiencies of marble waste during 20 min. calcination time in varying calcination temperatures

Considering that the calcination starts from the surface of the particle, the uniform calcination of large particles is more difficult than the smaller ones. In other words, the distance that the CO_2 will travel from inside the particle to the surface increases. Therefore, more time is required to calcine the larger particles (Boynton, 1980).

It is seen in Figure 4.7 that 20 minutes at 1000˚C is sufficient for almost complete calcination in marble wastes in both particle sizes for 98% and higher efficiencies. Although the particle size effect disappears during the calcination time of 20 minutes at 1000°C, which are the optimum conditions, the effect of the particle size on calcination efficiencies is observed at lower temperatures (900 and 950°C). At these lower temperature values, the calcination efficiency is higher in the smaller particle size intervals (-12.7+6.35 mm) than larger particle size intervals (-25.4+12.7 mm).

The XRD pattern of the lime of marble origin obtained from marble waste with the particle size range of -25.4+12.7 mm under the optimum calcination conditions (20 min., at 1000°C) is given in Figure 4.8. According to the XRD pattern, calcium oxide (CaO) is the main component of lime of marble origin, as expected.

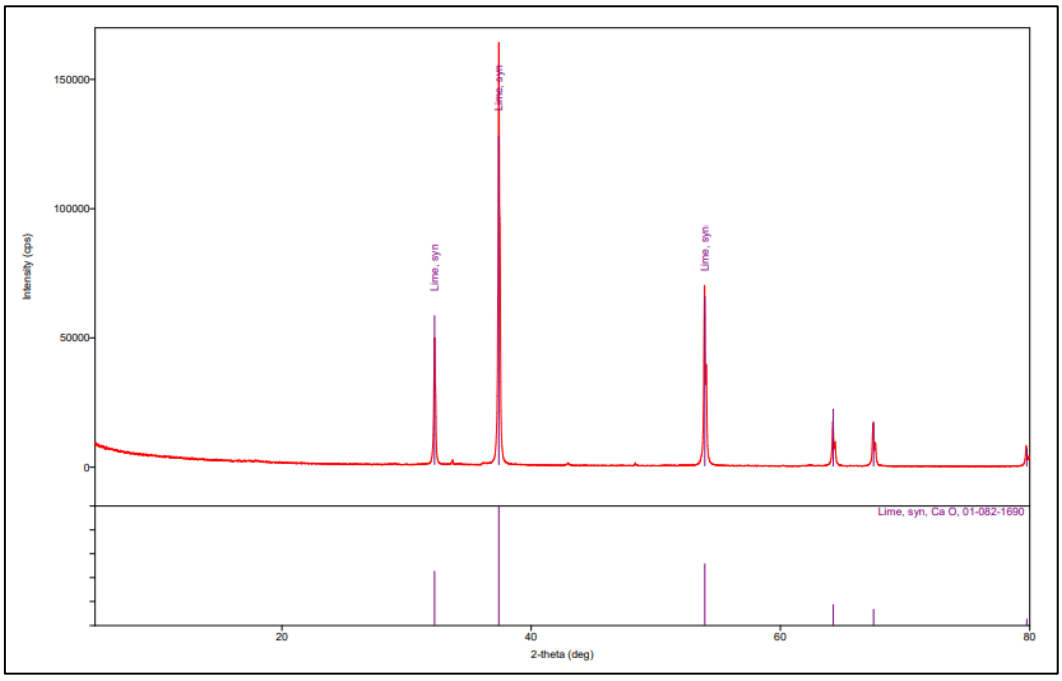

Figure 4.8 The XRD pattern of lime of marble origin

The effects of temperature for both size ranges, time, and particle size on the calcination of limestone are given in Figure A.1, Figure A.2, Figure A.3, and Figure A.4, respectively. The optimum conditions of limestone calcination are found to be 20 min. at 1000°C for both particle size ranges, which are the same optimum conditions as those of marble waste calcination.

The XRD pattern of lime of limestone origin obtained from limestone with the particle size range of -25.4+12.7 mm under the optimum conditions (20 min., 1000°C) is shown in Figure 4.9. This XRD pattern indicates that calcium oxide (CaO) is the main component of the lime of limestone origin.

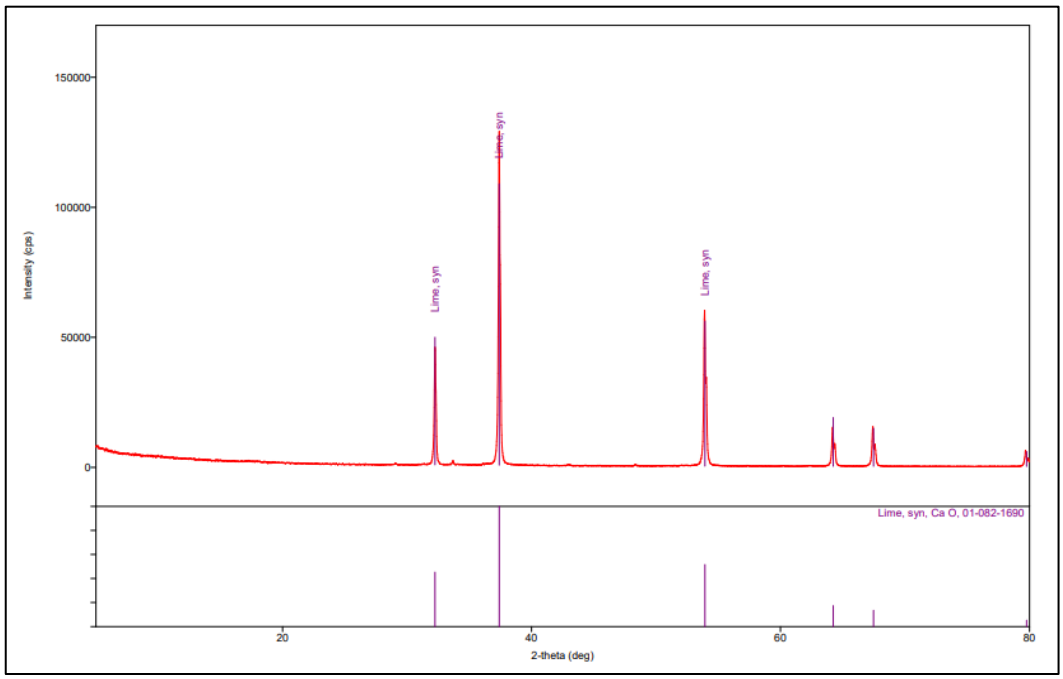

Figure 4.9 The XRD pattern of lime of limestone origin

4.2 Hydration Experiments

For the purpose of investigation of lime reactivity, the temperature profiles versus time recorded in the slaking experiments performed at three different lime to water ratios (1:3.5, 1:4.0, and 1:4.5 by weight) using limes of marble and limestone origins are given in Figure 4.10, Figure 4.11 and Figure 4.12. According to these figures, it

is clearly seen that the reaction temperature increases quite quickly. The decreasing slurry temperature from its highest value indicates an exothermic reaction is no longer occurring, and the lime particles react with water completely. In other words, there are little or no reactive residuals of lime remaining.

4.2.1 Effect of Lime to Water Ratio on the Hydration Temperature

As shown in Figure 4.10, the temperature profile of hydrated lime using lime to water ratio with 1:3.5 exhibits the same trend for both the lime of marble origin and lime of limestone origin. In the hydration of lime of marble origin process, the reaction temperature reaches its highest value at 86°C within 120 sec. Similarly, in the hydration of lime of limestone origin, the reaction temperature rises to 86.4°C within 120 sec. Since there is no temperature rise after around 260 sec. in the hydration of lime of marble waste, it is assumed that the reaction is over, and all the lime particles react with distilled water, forming $Ca(OH)_2$. In the hydration of lime of limestone origin, the temperature is steadily decreased after reaching its maximum value.

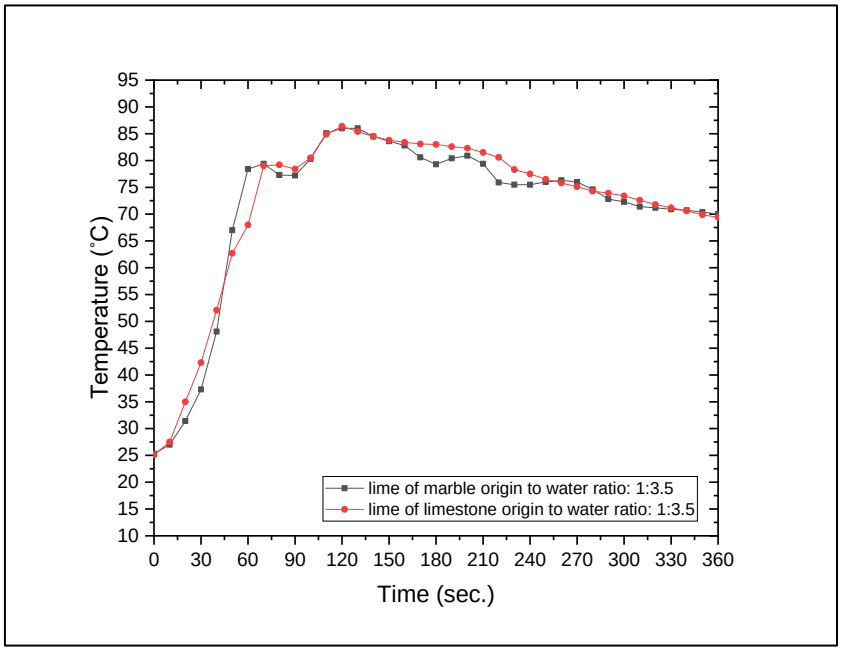

Figure 4.10 The temperature profiles of hydration of lime of marble and limestone origin prepared by 1:3.5 lime to water ratio

The temperature profile of hydration lime using lime to water ratio with 1:4.0 shows a slightly different trend for the lime of marble origin compared to lime of limestone origin (Figure 4.11). The rate of temperature increase in the hydration of lime of marble origin is higher than in the hydration of lime of limestone origin. While the temperature reaches 76.4°C within 70 seconds in the hydration of the lime of marble origin, the temperature reaches 75.3°C within 90 sec. in the hydration of the lime of limestone origin. The reaction is over after around 110 and 190 sec. for the hydration of limes of marble origin and limestone origin, respectively.

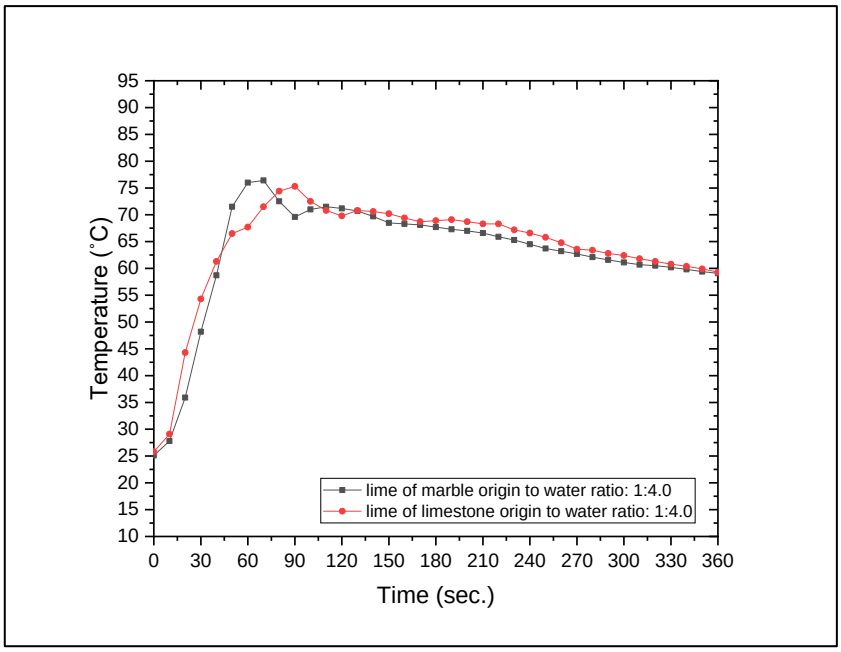

Figure 4.11 The temperature profiles of hydration of lime of marble and limestone origin prepared by 1:4.0 lime to water ratio

It is observed that the lime of marble origin reacts faster than the lime of limestone origin when the lime to water ratio is 1:4.5 (Figure 4.12). The temperature of hydration reaction using lime of marble origin could reach up to 73°C in 60 sec., whereas the temperature of hydration reaction using lime of limestone origin increases 71.6°C as its highest value within 80 sec. It is not observed any temperature rise after 100 and 120 sec. for the hydration of limes of marble origin and limestone origin, respectively.

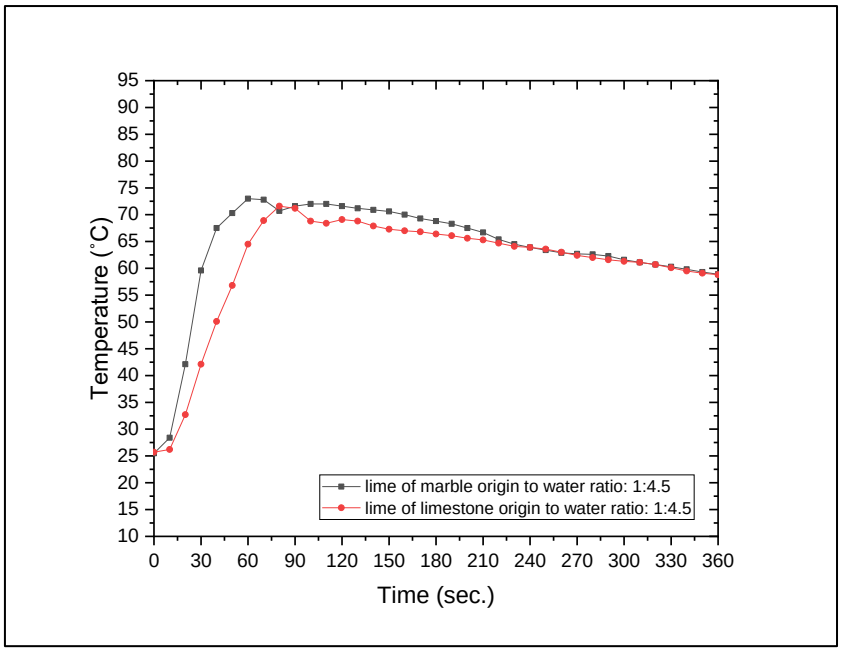

Figure 4.12 The temperature profiles of hydration of lime of marble and limestone origin prepared by 1:4.5 lime to water ratio

The cause of the fluctuations observed in the temperature profiles could be the subsequent reaction of lime particles that could not react with distilled water at the beginning of the reaction.

During the hydration reactions, reducing the limes to water ratio increases the rate of temperature rise and accelerates the rate of hydration since it will reduce the thermal capacity of the slurry (Oates, 1998).

Although temperatures around 100°C are desirable, it is difficult to slake properly at these high temperatures without causing safety issues and negative effects of agglomeration of calcium hydroxide particles. The hydration temperatures of 76°C to 85°C are more practicable for optimal operation in practice (Hassibi, 2009).

Moreover, it is known that the release of heat due to the exothermic reaction is different for different quality limes. In general, limes with high reactivity could be completely hydrated within 2-3 minutes (Hassibi, 2009).

In these regards, the lime to water ratio of 1:3.5 could be considered the optimum lime to water ratio in practice for the hydration application of lime of marble origin. Additionally, the temperature rise in the hydration of lime of marble origin reaches its maximum value within 2 minutes when the fluctuations are not taken into account. This is an indication that lime of marble waste is highly reactive.

The XRD pattern of milk of lime of marble origin, which was screened at 75 μm, is given in Figure 4.13. For the analysis, the milk of lime of marble origin was prepared as a 10% solid by weight and then dried at 90°C to obtain slaked lime in the powder form. In the XRD pattern, peaks of calcium hydroxide are observed dominantly, which indicates the complete hydration of lime of marble origin.

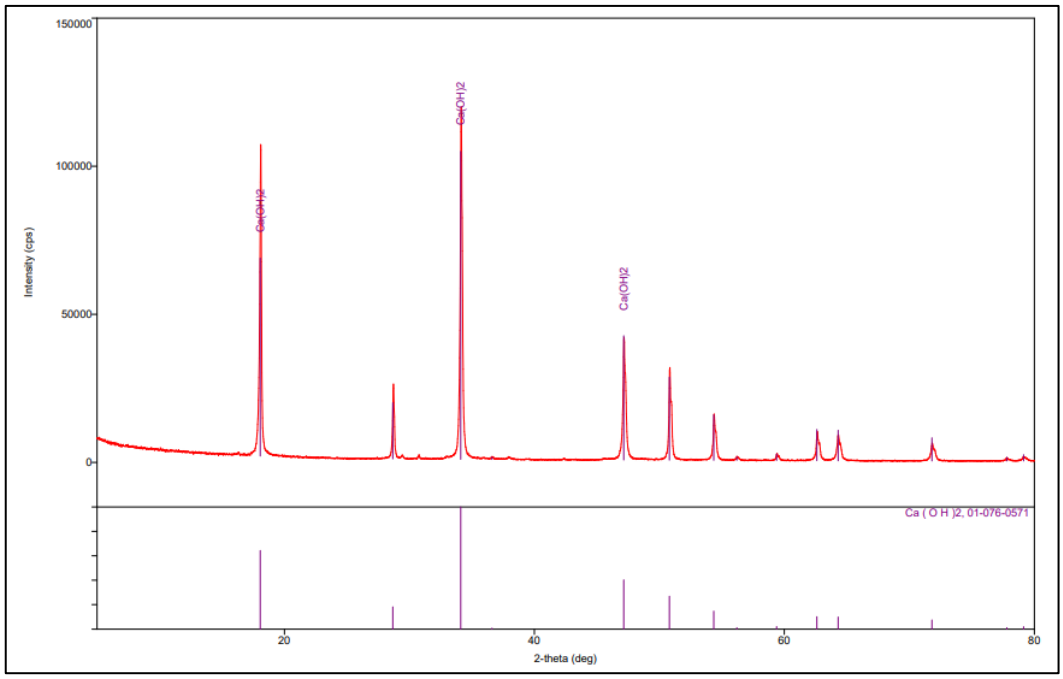

Figure 4.13 The XRD pattern of slaked lime of marble origin

The XRD pattern of milk of lime of limestone origin screened at 75 μm is shown in Figure 4.14. The milk of lime of limestone origin was prepared as a 10% solid by weight and dried at 90°C to obtain powdered slaked lime for the analysis. Similar to the XRD pattern of milk of lime of marble origin, peaks of calcium hydroxide are observed as the main mineral component.

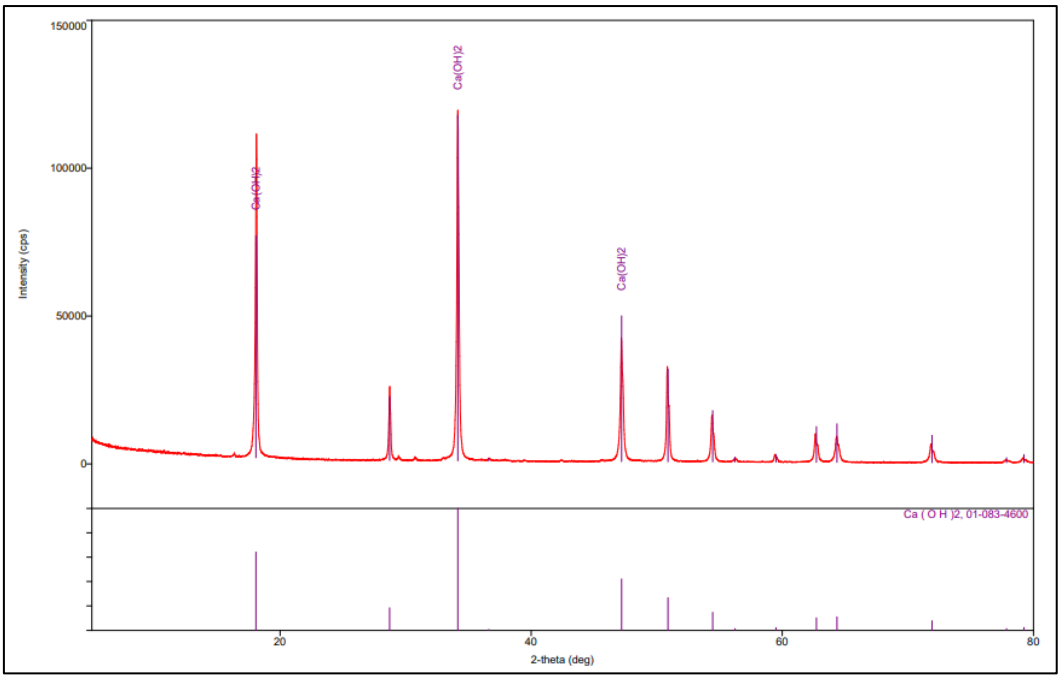

Figure 4.14 The XRD pattern of slaked lime of limestone origin

4.3 Carbonation Experiments

As a final stage of PCC production, milk of limes of marble and limestone origins with 5% and 10% $Ca(OH)_2$ concentrations was precipitated by using compressed CO_2 in the autoclave. The constant CO_2 pressure values of 5 and 10 bar were used during the experiments.

The temperature rise is expected during the reaction since the precipitation reaction is exothermic. This rise will end with the precipitation of $Ca(OH)_2$ suspension as $CaCO_3$ crystals. In the production of PCCs from marble waste and limestone, the maximum temperature values measured in the autoclave during the precipitation reaction and the carbonation times, that pass until the maximum temperature was reached, are given in Table 4.1 and Table 4.2. After these maximum temperature values reached, it was observed that the temperature values were decreased rapidly as the reaction ended.

Additionally, at the end of each reaction, the pH value of the milk of lime suspension, which was 12-12.5 at the beginning of the reaction, was measured in the range of 7-8 by a litmus test paper. This decrease in the pH value is also an indicator of the complete reaction.

Table 4.1 The carbonation times and the maximum temperature values during the production of PCC from marble waste

Concentration of $Ca(OH)_2$	5 %		10 %	
CO_2 pressure	5 bar	10 bar	5 bar	10 bar
Carbonation time	20 min.	8 min.	30 min.	14 min.
The maximum temperature value reached during the reaction	31°C	30°C	34°C	35°C

Table 4.2 The carbonation times and the maximum temperature values during the production of PCC from limestone

Concentration of $Ca(OH)_2$	5 %		10 %	
CO_2 pressure	5 bar	10 bar	5 bar	10 bar
Carbonation time	18 min.	7 min.	27 min.	15 min.
The maximum temperature value during the reaction	30°C	32°C	34°C	34°C

It is seen from the above tables that under high CO_2 pressure (10 bar) and low $Ca(OH)_2$ concentration (5 %), carbonation times of $CaCO_3$ particles are less than 10 minutes for the experiments conducted by using milk of lime of marble and limestone origins. In contrast, carbonation time almost doubles as the concentration increases to 10% under the 10 bar CO_2 pressure. Moreover, under low CO_2 pressure (5 bar), the reaction at low $Ca(OH)_2$ concentration (5 %) occurs faster than the reaction at higher $Ca(OH)_2$ concentration (10 %).

The particle size distribution of PCCs is an important characteristic for the applications, mentioned in Section 2.3.2.

According to the particle size distribution results (given from Fig. C.1 to Fig. C.8) of PCCs, the medians of the volume distribution (d(0.5)) of samples are shown in Table 4.3.

Table 4.3 The d(0.5) size of PCC produced from marble waste and limestone

Concentration of $Ca(OH)_2$	5 %		10 %	
CO_2 pressure	5 bar	10 bar	5 bar	10 bar
d(0.5) size of PCC produced from marble waste	8.226 μm	7.152 μm	10.222 μm	9.270 μm
d(0.5) size of PCC produced from limestone	9.740 μm	8.076 μm	11.051 μm	9.641 μm

d(0.5) is the size of particle below that 50% of the sample lies. It is observed that the d(0.5) size of PCC produced from marble waste is slightly smaller than the d(0.5) size of PCC produced from limestone. It means that the median diameters of the $CaCO_3$ crystals (marble origin) are smaller than the $CaCO_3$ crystals (limestone origin) under the studied conditions of PCC production. Although this difference is very small, the same results were obtained in each experiment.

Surface weighted mean sizes (D[3.2]) of PCCs obtained from marble waste and limestone are given in Table 4.4. There is no significant mean size difference between the PCCs produced from marble waste and limestone.

Table 4.4 The mean size of PCC produced from marble waste and limestone

Concentration of $Ca(OH)_2$	5 %		10 %	
CO_2 pressure	5 bar	10 bar	5 bar	10 bar
Mean size of PCC produced from marble waste	3.030 μm	3.116 μm	3.558 μm	3.920 μm
Mean size of PCC produced from limestone	3.368 μm	3.682 μm	3.522 μm	3.366 μm

The XRD patterns of PCC products are shown in Figure 4.15 and Figure 4.16.

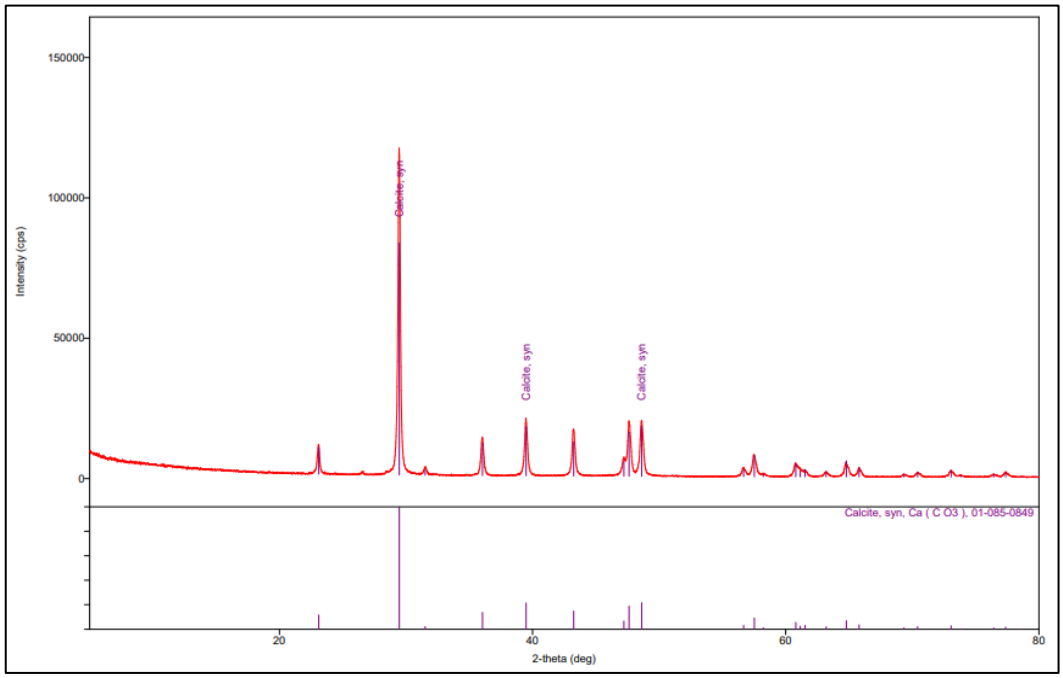

Figure 4.15 The XRD pattern of PCC produced from marble waste

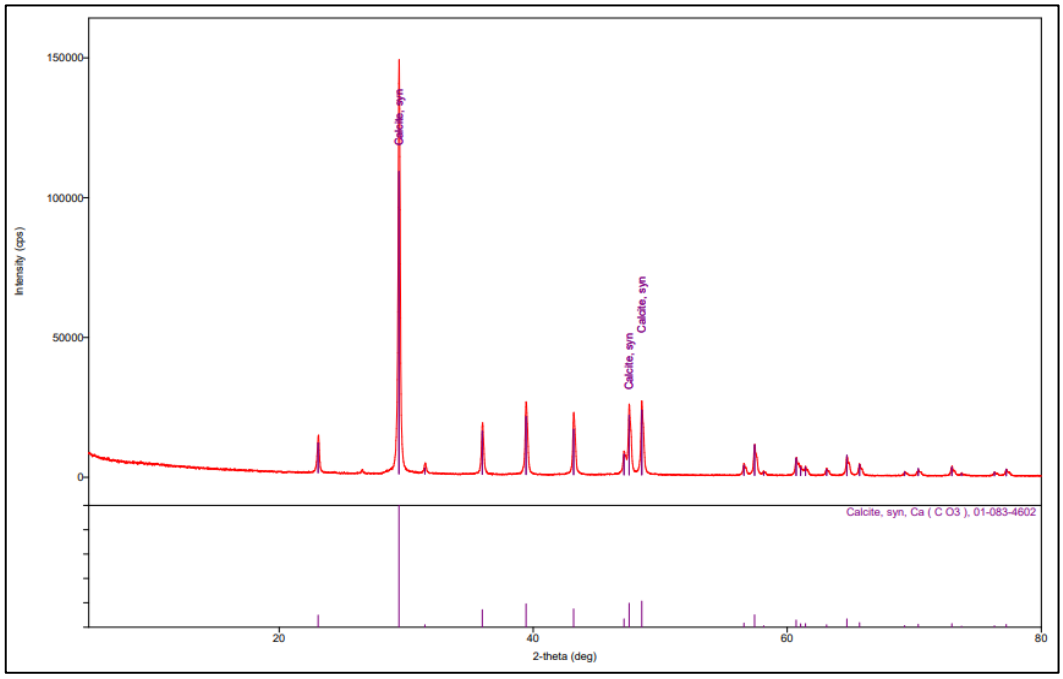

Figure 4.16 The XRD pattern of PCC produced from limestone

For the XRD analysis, the powdered PCC samples produced at 5 bar CO_2 pressure and using 5% $Ca(OH)_2$ suspension were used. It is identified in the XRD patterns that calcium carbonate ($CaCO_3$) is the major component of PCC products.

4.3.1 Color Analyses of PCCs

The difference between the colors of the PCCs produced by the carbonation route could be distinguished in the photo taken in daylight (shown in Figure 4.17). It is seen that the color of PCCs obtained from marble origin is more yellowish than the color of PCCs obtained from limestone origin.

Figure 4.17 Produced PCCs from marble waste and limestone origin

A whiteness value (relative to $BaSO_4$), whiteness and yellowness indexes of produced PCCs are given in Table 4.5. Whiteness could be defined as the attribution of a substance's color is assessed to be close to the reference white (ASTM, 2015). It is seen that the whiteness value (89.89) of PCCs obtained from marble waste is low compared to other PCCs (95.68 for PCCs obtained from limestone and 97.26 for commercial PCCs)

In order to determine the degree to which PCCs color shifts away from a reference white, the whiteness and yellowness indexes are used. These indexes are the numbers computed from colorimetric data. The yellowness index is described as the change in color of the studied sample from white to yellow, whereas the whiteness index is defined as the degree of departure of a sample color from that of the reference white (ASTM, 2015). It is observed that the yellowness index of PCCs produced from marble waste is relatively high when compared to commercial PCCs and PCCs produced from limestone. In addition, it is clearly seen from the below table that the whiteness index of PCCs produced from marble waste is at the lowest value through the other PCCs.

Table 4.5 The whiteness and yellowness indexes of PCCs

	Whiteness (relative to $BaSO_4$)	Whiteness Index	Yellowness Index
PCC produced from marble waste	89.89	74.662	7.364
PCC produced from limestone	95.68	93.015	1.921
PCC produced by Adaçal Industrial Minerals Co.	97.26	95.400	1.541

The color data of PCCs from the analyzer, including the CIE (International Commission on Illumination) X, Y, and Z color spaces (the tristimulus values) and the coefficient used in the index calculations, are given in Table C.1..

4.3.2 Morphological Analyses of PCCs

SEM images of PCCs are shown in Figure 4.18 and Figure 4.19. The rhombohedral calcite crystals are observed in both samples with a narrow size range distribution. The powdered PCC samples precipitated by using 5% $Ca(OH)_2$ concentration at 5 bar CO_2 pressure were used for the XRD analysis.

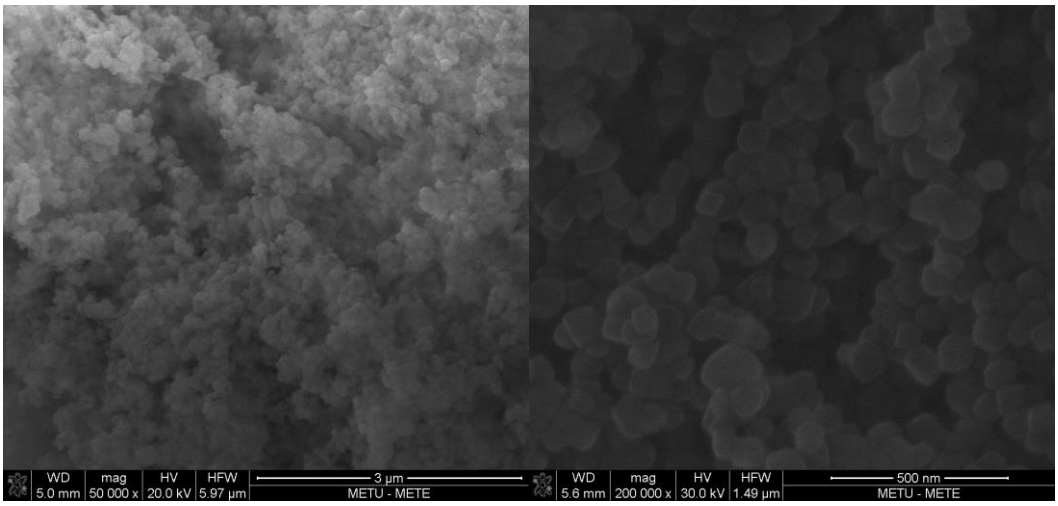

Figure 4.18 Scanning electron microscopy (SEM) images of PCCs produced from marble waste

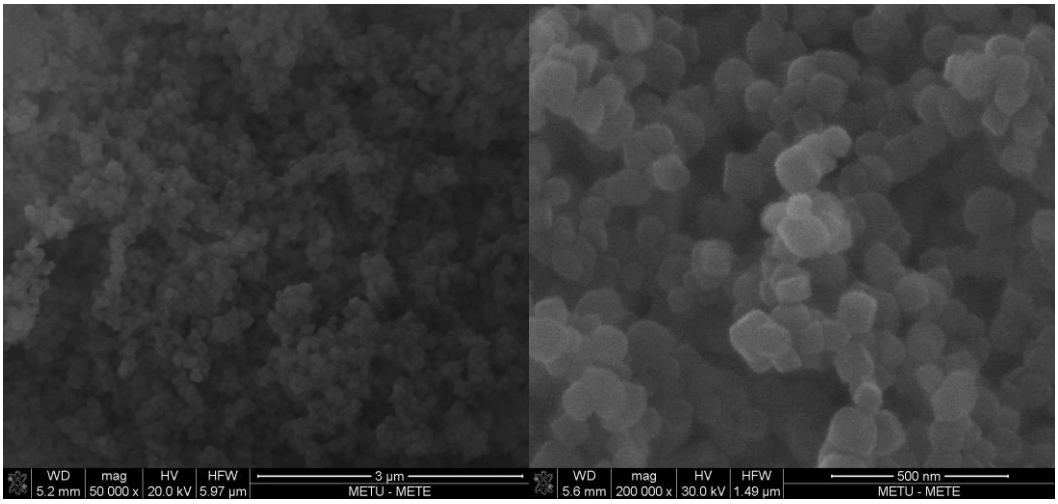

Figure 4.19 Scanning electron microscopy (SEM) images of PCCs produced from limestone

CHAPTER 5

CONCLUSIONS AND RECOMMENDATIONS

The production of precipitated calcium carbonate from marble waste was investigated in this study. The production stages include calcination, hydration, carbonation. The following conclusions and recommendations could be drawn based on the experimental results of the precipitated calcium carbonate production.

In the calcination experiments, it was indicated that the marble waste and limestone samples exhibit the same calcination characteristic, even though they are rocks of different origins. In order to achieve at least 98% efficiency, the optimum calcination conditions were found to be 20 minutes at 1000°C for the particle size ranges of -25.7+12.7 mm and -12.7+6.35 mm. The stone quality (degree of crystallinity, the tendency to decrepitate, and impurities present in stone) can vary in a wide range. Therefore, it should be noted that the optimum calcination temperature could only be determined by experimentation for studied limestone and marble rocks. The generalization of optimum calcination temperature is not recommended. It is also noticed that depending on the calcination temperature, particle size range and retention time are changeable parameters.

In the hydration of the limes of marble and limestone origin, the reactivity of limes could be assumed as the same since the rate of temperature increase is almost the same.

According to carbonation experiments, PCC obtained from marble waste and PCC obtained from limestone were successfully produced under the same conditions. It is indicated that the median sizes and surface weighted mean sizes of the PCC particles produced from marble waste were the same as the PCC product produced from limestone under the same precipitation conditions.

In the characterization of PCC produced from the lime of marble origin, it was observed that whiteness value and whiteness index were not sufficient in addition to the high yellowness index. It is noticed that marble wastes were not subjected to any pre-washing process in this study. Therefore, the effect of this situation on the color of the produced PCC product should be considered for further investigations. Besides these, the contents causing the color of PCC produced from marble waste and operational conditions, if any, could be studied.

The obtained morphology of produced PCCs was rhombohedral. In further studies, the effects of temperature on PCC morphology could be studied in order to produce PCCs with different morphology than rhombohedral.

In conclusion, it is possible to produce PCC from marble waste with a narrow size range distribution. Lime, milk of lime, and PCCs of marble origin, which are the products of calcination, hydration, and carbonation stages, could be produced under the same conditions as those of limestone origin.

REFERENCES

Afridi, S. K., Bhatty, M. B., Ahmed, A. S., Saeed, M. T., & Ahmad, S. (2008). Experimental Study of Calcination-Carbonation Process for the Production of Precipitated Calcium Carbonate. J. Chem. Soc. Pak., 30(4).

Altun, N. E. (2016). Reactivity of marble wastes for potential utilization in wet flue gas desulphurization. Physicochemical Problems of Mineral Processing, 52(1), 497–509.

ASTM. (2015). Standard Practice for Calculating Yellowness and Whiteness Indices from Instrumentally Measured Color Coordinates. Annual Book of ASTM Standards, 06(C), 1–6. http://www.astm.org/cgi-bin/resolver.cgi?E313-15e1

Belete, T. T. (2019). Evaluation of (plasma-assisted) decomposition of transition metals doped CaCO3 for CO2 capture and conversion Evaluation of (Plasma-assisted) Decomposition of Transition Metals Doped CaCO3 for CO2 Capture and Conversion.

Bilgin, N., Yeprem, H. A., Arslan, S., Bilgin, A., Günay, E., & Maroglu, M. (2012). Use of waste marble powder in brick industry. Construction and Building Materials, 29, 449–457. https://doi.org/10.1016/j.conbuildmat.2011.10.011

Bilgin, Ö., & Koç, E. (2013). Mermer Madenciliğinde Çevresel Etkiler. Madencilik Türkiye Dergisi.

Boateng, A. (2013). Rotary Kilns Transport Pheenomena and Trasport Processes.

Boggs, S. J. (2009). Petrology of Sedimentary Rocks (Second). Cambridge University Press.

Bowles, O. (1916). The Technology of Marble Quarrying. Washington Goverment Printing Office.

Boynton, R. S. (1980). Chemistry and Technology of Lime and Limestone (& J. W. & Sons (eds.)).

Brown C.A., Compton R.G., Narramore C.A., The kinetics of calcite dissolution/precipitation, J. Colloid Interface Sci. 160 (2) (1993) 372–379.

Chen Z., Nan Z. (2011). Controlling the polymorph and morphology of CaCO3 crystals using surfactant mixtures. J Colloid Interface Sci 358(2):416–422

Chorney, J. L. (2019). Calcination. In SME Mineral Processing & Extractive Metallurgy Handbook (pp. 1445–1452).

Chukwudebelu J.A., Igwe C.C., Taiwo O.E., & Tojola O.B. (2013). Recovery of pure slaked lime from carbide sludge: Case study of Lagos state, Nigeria. Afr. J. Environ. Sci. Technol. 7, 490-495.

Cox, F.C., Bridge, Mc.C. & Hull, J.H. (1977). Procedures for the assessment of limestone resources. Institute of Geological Science, Mineral Assessment Report 30, 20pp.

Çelik, M.Y., (1996). Mermer Artıklarının (Parça Tozların) Değerlendirilmesi. A.K.Ü. Fen Bilimleri Enstitüsü Yüksek Lisans Tezi, Afyon, 119pp

Çetin, T. (2003a). Türkiye Mermer Potansiyeli , Üretimi ve İhracatı. GÜ, Gazi Eğitim Fakültesi Dergisi, 3(December), 243–256.

Çetin, T. (2003b). Türkiye Mermer Potansiyeli , Üretimi ve İhracatı Marble Potential , Production and Export of Turkey. Production, 3(January 2003), 243–256.

D'Haese M., Langouche F., Van Puyvelde P. (2013). On the effect of particle size, shape, concentration, and aggregation on the flow- induced crystallization of polymers. Macromolecules 46(9):3425–3434

Dogan O., Yıldırım M. (2008). The investigation of recovery conditions of precipitated calcium carbonate from Afsin – Elbistan power plant fly ashes. Cukurova Univ. J. Sci. Inst. 17, 95-102.

Domingo, C., Loste, E., Gómez-Morales, J., García-Carmona, J., & Fraile, J. (2006). Calcite precipitation by a high-pressure CO2 carbonation route. Journal of Supercritical Fluids, 36(3), 202–215. https://doi.org/10.1016/j.supflu.2005.06.006

Elçi, H., Hacımustafaoğlu, R., Yılmaz, M., & Yılmaz, Ö. (2017). Ham Madde Kaynağı Olarak Doğal Taş Artıkları, Torbalı - İzmir Örneği. Uluslararası Madencilik ve Çevre Sempozyumu-ISME2017, October, 1029–1043.

El-Sherbiny S., El-Sheikh S., Barhoum A. (2015) Preparation and modification of nano calcium carbonate filler from waste marble dust and commercial limestone for papermaking wet end application. Powder Technol 279:290–300

Erdogan, N., & Eken, H. A. (2017). Precipitated Calcium carbonate production, synthesis and properties. Physicochemical Problems of Mineral Processing, 53(1), 57–68. https://doi.org/10.5277/ppmp170105

Grossou-Yalta, M., Mavroyiannis, J., & Chalkiopoulou, F. (2003). Waste minimization in mineral and rocks exploitation by integrated management and production of value added materials. Sustainable Waste Management, Proceedings of the International Symposium, 253–264.

Hassibi, M. (2009). An overview of lime slaking and factors that affect the process, 1st Revision, Presenting to the 3rd International Sorbalit Symposium, 1999, New Orleans.

Hebhoub, H., Aoun, H., Belachia, M., Houari, H., & Ghorbel, E. (2011). Use of waste marble aggregates in concrete. Construction and Building Materials, 25(3), 1167–1171. https://doi.org/10.1016/j.conbuildmat.2010.09.037

Hubbe M.A., Gill R.A. (2016) Fillers for papermaking: a review of their properties, usage practices, and their mechanistic role. BioRe- sources 11(1):2886–2963

Jimoh, O. A., Ariffin, K. S., Hussin, H. Bin, & Temitope, A. E. (2018). Synthesis of precipitated calcium carbonate: a review. Carbonates and Evaporites, 33(2), 331–346. https://doi.org/10.1007/s13146-017-0341-x

Karaca, Z., Pekin, A., & Deliormanlı, A. H. (2012). Classification of dimension stone wastes. Environmental Science and Pollution Research, 19(6), 2354–2362. https://doi.org/10.1007/s11356-012-0745-z

Karahan, D. S. (2018). Dünyada ve Türkiye'de Doğal Taşlar. In MTA Fizibilite Etütleri Daire Başkanlığı.

Ketin, İ. (1984). Türkiye Jeolojisine Genel Bir Bakış. İstanbul: İst. Tek. Üniv. Vakfı Yay. No:32

Koutsoukos, P. G., & Chen, T. (2010). Calcium Carbonate: Polymorphs Stabilization in the Presence of Inhibitors. In The Science and Technology of Industrial Water Treatment.

Kumar, G. S., Ramakrishnan, A., & Hung, Y.-T. (2007). Lime Calcination. ChemInform, 38(24). https://doi.org/10.1002/chin.200724211

Kun, N. (2013) Mermer jeolojisi ve teknolojisi, Genişletilmiş 2. Baskı, 222 s., İzmir.

Leontakianakos G., Baziotis I., Profitis E., Chatzitheodoridis E., Tsimas S. (2013). Assessment of the quality of calcination of marbles from Thassos Island using Raman Spectroscopy and X-Ray Diffraction. In Proceedings proceedings of the 13th international congress, vol 47

Lhoist Group, (n.d.). https://www.lhoist.com/want-know-more-about%E2%80%A6, last visited on December 2021.

Liguori, V., Rizzo, G., & Traverso, M. (2008). Marble quarrying: An energy and waste intensive activity in the production of building materials. WIT

Transactions on Ecology and the Environment, 108(May), 197–207.

Maden ve Petrol İşleri Genel Müdürlüğü (MAPEG). (2020). https://www.mapeg.gov.tr/maden_istatistik.aspx, last visited on September 2021.

Mantilaka, M. M. M. G. P. G., Karunaratne, D. G. G. P., Rajapakse, R. M. G., & Pitawala, H. M. T. G. A. (2013). Precipitated calcium carbonate/poly(methyl methacrylate) nanocomposite using dolomite: Synthesis, characterization and properties. Powder Technology, 235, 628–632. https://doi.org/10.1016/j.powtec.2012.10.048

MEGEP. (2008). Makina Teknolojisi, Mermer Blok Üretimi.

Mehta, D., Paliwal, D., & Sankhla, V. S. (2020a). Marble Waste Management for Protection of Ecology and Environment. International Journal of Innovative Science, Engineering & Technology, 7(7), 154–169.

Mehta, D., Paliwal, D., & Sankhla, V. S. (2020b). Study of Marble Waste and Its Utilization.pdf. International Research Journal of Engineering and Technology (IRJET), 7(7).

Miller, M.M. (2003) Lime: 2003 minerals yearbook

Minerals Technologies Inc., (2021). https://www.mineralstech.com/business-segments/specialty-minerals/paper-pcc/precipitated-calcium-carbonate-(pcc), last visited on Septemper 2021.

Mitchell, C J. (2011). High purity limestone quest. Industrial Minerals, 531. 48-51

MTA, (1966). Türkiye mermer envanteri, MTA Enstitüsü, Yayın No: 134, Ankara

Mullin, J.W. (1997) Crystallization, Butterwoth-Heinemann, Oxford, UK

Muslim, W. A., & Mustafa, A. M. K. (2015). Preparation of Precipitated Calcium Carbonate. Iraqi Bulletin of Geology and Mining, 11(2), 123–138.

Murray. J.A. (1954), J. Am. Ceram. Soc. 37, No 7,323-328.

Oates, J. A. H. (1998). Lime and Limestone. In Wiley-VCH. https://doi.org/10.1002/9783527612024

Said A., Mattila H-P., Ja¨rvinen M., Zevenhoven R. (2013) Production of precipitated calcium carbonate (PCC) from steelmaking slag for fixation of CO2. Appl Energy 112:765–771

Sanders, J. E., & Friedman, G. M. (1967). Chapter 5 Origin and Occurrence of Limestones. Developments in Sedimentology, 9(PART A), 169–265. https://doi.org/10.1016/S0070-4571(08)71113-0

Souto, E.C.S. Damasceno, J.J.R. Hori, C.E., 2008. Study of operational conditions for the precipitated calcium carbonate production. Materials Science Forum, 591-593, 526-530.

Teir, S., Eloneva, S., Fogelholm, C. J., & Zevenhoven, R. (2007). Dissolution of steelmaking slags in acetic acid for precipitated calcium carbonate production. Energy, 32(4), 528–539. https://doi.org/10.1016/j.energy.2006.06.023

Teir, S., Eloneva, S., & Zevenhoven, R. (2005). Production of precipitated calcium carbonate from calcium silicates and carbon dioxide. Energy Conversion and Management,46(18–19),2954–2979. https://doi.org/10.1016/j.enconman.2005.02.009

Tucker, M. E. (2001). Sedimentary petrology. An introduction to the orgin of sedimentary rocks. In Blackwell Science Publication: Vol. 2nd Ed.

Ukrainczyk, M., Kontrec, J., Babić-Ivančić, V., Brečević, L., & Kralj, D. (2007). Experimental design approach to calcium carbonate precipitation in a semicontinuous process. Powder Technology, 171(3), 192–199.

https://doi.org/10.1016/j.powtec.2006.10.046

US Environmental Protection Agency (EPA). (November 12,2020). https://www.epa.gov/recycle/recycling-basics, last visited on September 2021.

World Bank, (2006). Pakistan Growth and Export Competitiveness (Issues 35499-PK).

APPENDICES

A. Experimental Results of Calcination

Table A.1 The calcination efficiencies of marble waste

Efficiency (%)						
Temperature	900˚C		950˚C		1000˚C	
Size (mm)	-12.7+6.35	-25.4+12.7	-12.7+6.35	-25.4+12.7	-12.7+6.35	-25.4+12.7
Time(min)						
10	76.88	43.12	96.43	81.1	97.60	93.29
20	86.6	55.84	97.15	88.87	98.54	98.11
30	97.02	68.99	97.39	97.10	98.93	98.38
60	97.36	92.16	98.87	97.67	99.05	99.07
90	97.82	98.18	98.93	98.45	99.17	99.09
120	99.05	98.86	99.24	99.07	99.32	99.13

Table A.2 The calcination efficiencies of limestone

Efficiency (%)						
Temperature	900˚C		950˚C		1000˚C	
Size (mm)	-12.7+6.35	-25.4+12.7	-12.7+6.35	-25.4+12.7	-12.7+6.35	-25.4+12.7
Time(min)						
10	77.23	43.26	96.74	79.41	97.65	91.76
20	90.50	55.98	97.26	88.58	98.62	98.42
30	96.47	68.95	98.10	98.33	98.87	98.35
60	98.17	90.26	98.56	99.07	98.99	99.09
90	98.54	97.93	99.45	98.97	99.04	99.09
120	98.98	98.74	99.07	99.01	99.11	99.14

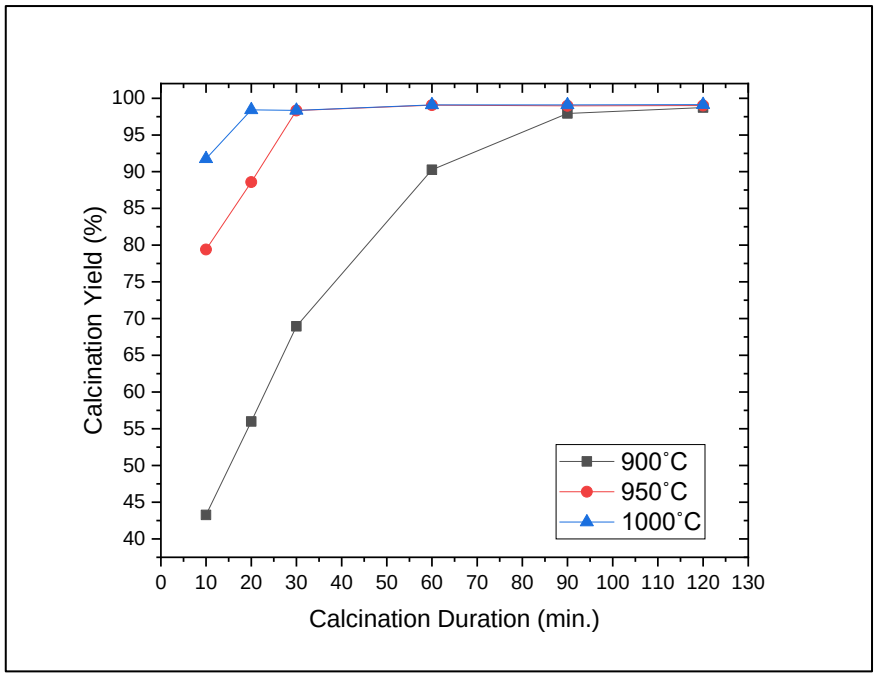

Figure A.1 The calcination efficiencies of limestone with a particle size interval of -25.4+12.7 mm in varying calcination temperatures

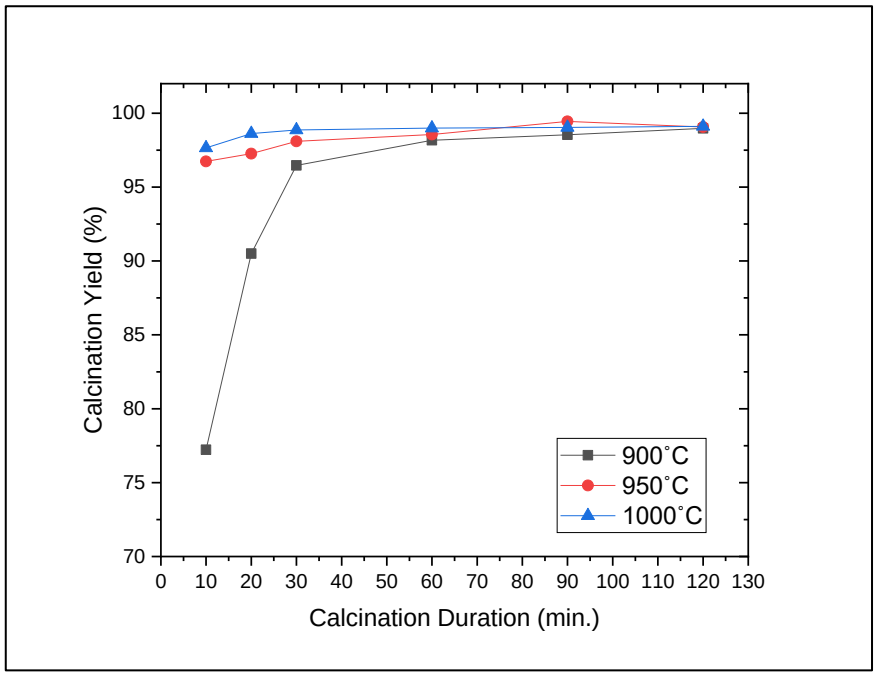

Figure A.2 The calcination efficiencies of limestone with a particle size interval of -12.7+6.35 mm in varying calcination temperatures

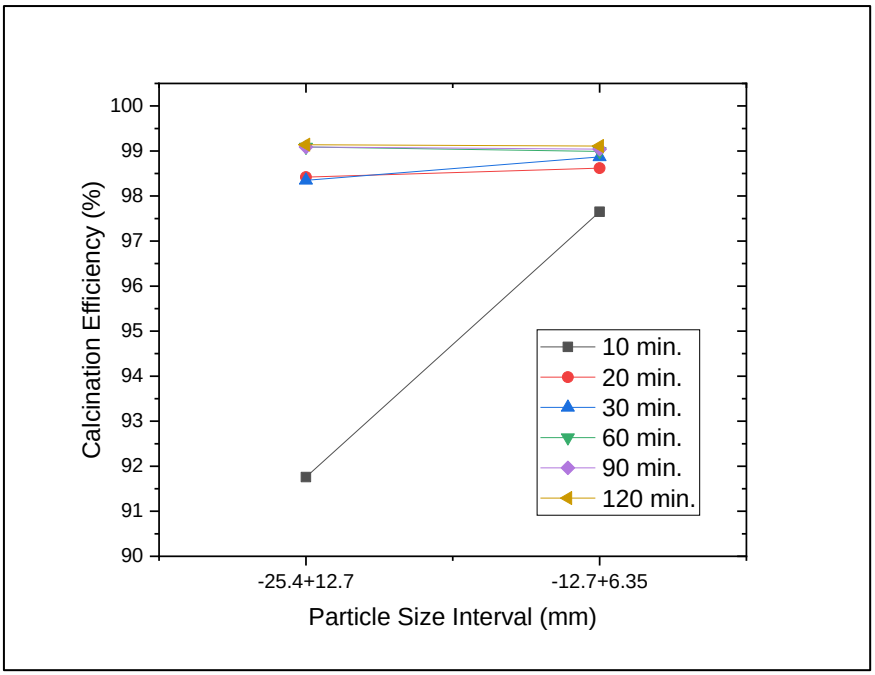

Figure A.3 The calcination efficiencies of limestone at 1000˚C in varying particle size ranges

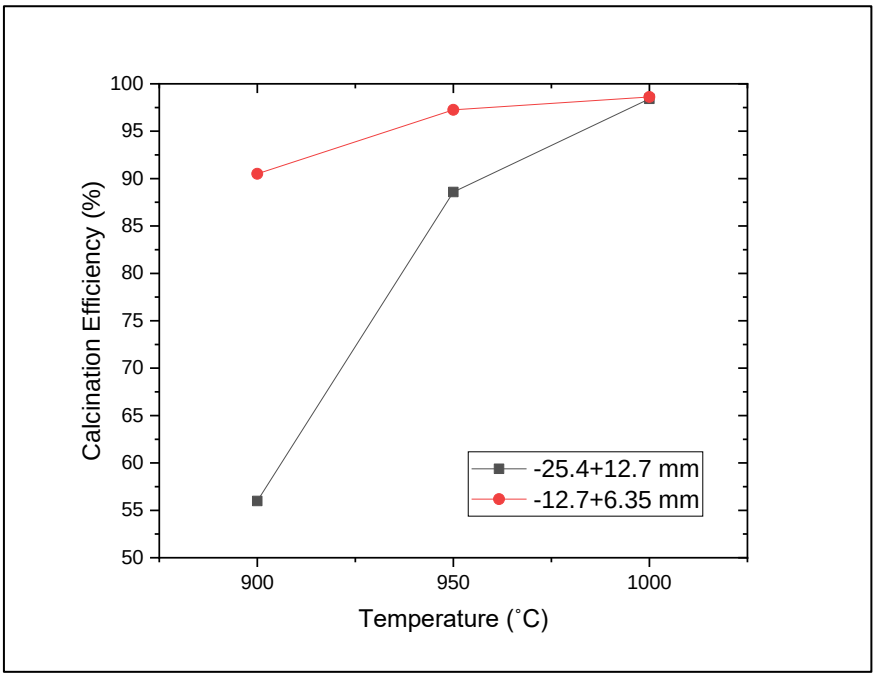

Figure A.4 The calcination efficiencies of limestone during 20 min. calcination time in varying calcination temperatures

B. Experimental Results of Hydration of Lime

Table B.1 The hydration gradients of hydration of lime of marble and limestone origin prepared by 1:3.0 lime to water ratio

Time (sec.)	Lime of Marble Origin	Lime of Limestone Origin	Time (sec.)	Lime of Marble Origin	Lime of Limestone Origin
	Temperature (°C)			Temperature (°C)	
0	25.3	25.2	190	80.4	82.6
10	27	27.5	200	80.9	82.3
20	31.4	35	210	79.4	81.5
30	37.3	42.3	220	75.9	80.6
40	48.1	52.1	230	75.5	78.3
50	67	62.7	240	75.5	77.5
60	78.4	68	250	76	76.5
70	79.4	79	260	76.3	75.8
80	77.3	79.2	270	76	75.1
90	77.2	78.4	280	74.6	74.3
100	80.3	80.5	290	72.8	73.9
110	85.1	84.9	300	72.3	73.4
120	86	86.4	310	71.4	72.6
130	86	85.4	320	71.2	71.8
140	84.5	84.5	330	70.9	71.2
150	83.6	83.8	340	70.7	70.6
160	82.8	83.4	350	70.4	69.9
170	80.6	83.1	360	70	69.4
180	79.3	83			

Table B.2 The hydration gradients of hydration of lime of marble and limestone origin prepared by 1:4.0 lime to water ratio

Time (sec.)	Lime of Marble Origin	Lime of Limestone Origin	Time (sec.)	Lime of Marble Origin	Lime of Limestone Origin
	Temperature (°C)			Temperature (°C)	
0	25.1	25.8	190	67.3	69.1
10	27.8	29.1	200	67	68.7
20	35.9	44.3	210	66.6	68.3
30	48.2	54.3	220	65.9	68.3
40	58.7	61.3	230	65.3	67.2
50	71.5	66.5	240	64.5	66.6
60	76	67.7	250	63.7	65.8
70	76.4	71.5	260	63.2	64.8
80	72.5	74.4	270	62.7	63.6
90	69.6	75.3	280	62.1	63.4
100	71	72.5	290	61.6	62.8
110	71.5	70.8	300	61.1	62.4
120	71.2	69.8	310	60.7	61.8
130	70.7	70.8	320	60.5	61.3
140	69.7	70.6	330	60.2	60.8
150	68.5	70.2	340	59.8	60.4
160	68.3	69.4	350	59.4	59.9
170	68.1	68.7	360	59.1	59.3
180	67.7	68.9			

Table B.3 The hydration gradients of hydration of lime of marble and limestone origin prepared by 1:4.5 lime to water ratio

Time (sec.)	Lime of Marble Origin	Lime of Limestone Origin	Time (sec.)	Lime of Marble Origin	Lime of Limestone Origin
	Temperature (°C)			Temperature (°C)	
0	25.5	25.6	190	68.3	66.1
10	28.4	26.2	200	67.5	65.6
20	42.1	32.7	210	66.7	65.3
30	59.6	42.1	220	65.4	64.7
40	67.5	50.1	230	64.5	64.1
50	70.3	56.8	240	63.9	63.9
60	73	64.5	250	63.4	63.6
70	72.8	68.9	260	62.9	63
80	70.7	71.6	270	62.7	62.4
90	71.6	71.2	280	62.6	62
100	72	68.8	290	62.3	61.6
110	72	68.4	300	61.6	61.3
120	71.5	69.1	310	61.1	61.1
130	71.2	68.8	320	60.7	60.7
140	70.9	67.9	330	60.3	60.1
150	70.6	67.3	340	59.8	59.5
160	70	67	350	59.3	59.1
170	69.3	66.8	360	58.9	58.8
180	68.8	66.4			

C. Experimental Results of Carbonation

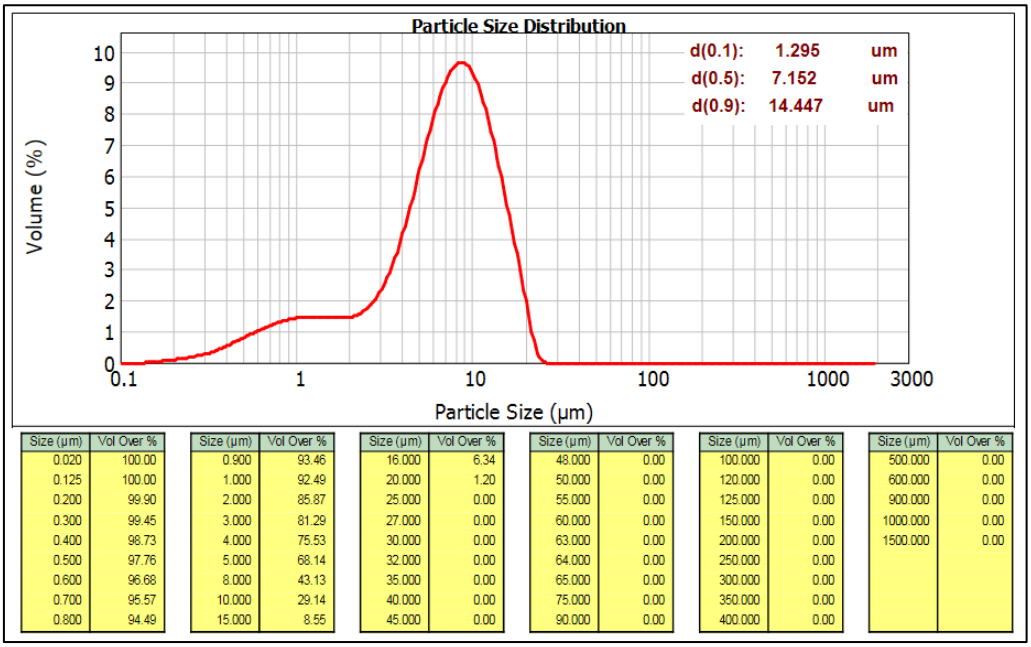

Size (µm)	Vol Over %	Size (µm)	Vol Over %	Size (µm)	Vol Over %	Size (µm)	Vol Over %	Size (µm)	Vol Over %	Size (µm)	Vol Over %
0.020	100.00	0.900	93.46	16.000	6.34	48.000	0.00	100.000	0.00	500.000	0.00
0.125	100.00	1.000	92.49	20.000	1.20	50.000	0.00	120.000	0.00	600.000	0.00
0.200	99.90	2.000	85.87	25.000	0.00	55.000	0.00	125.000	0.00	900.000	0.00
0.300	99.45	3.000	81.29	27.000	0.00	60.000	0.00	150.000	0.00	1000.000	0.00
0.400	98.73	4.000	75.53	30.000	0.00	63.000	0.00	200.000	0.00	1500.000	0.00
0.500	97.76	5.000	68.14	32.000	0.00	64.000	0.00	250.000	0.00		
0.600	96.68	8.000	43.13	35.000	0.00	65.000	0.00	300.000	0.00		
0.700	95.57	10.000	29.14	40.000	0.00	75.000	0.00	350.000	0.00		
0.800	94.49	15.000	8.55	45.000	0.00	90.000	0.00	400.000	0.00		

Figure C.1 The result of particle size analysis of PCC product (marble waste origin) produced by using 5% $Ca(OH)_2$ concentration at 10 bar CO_2 pressure

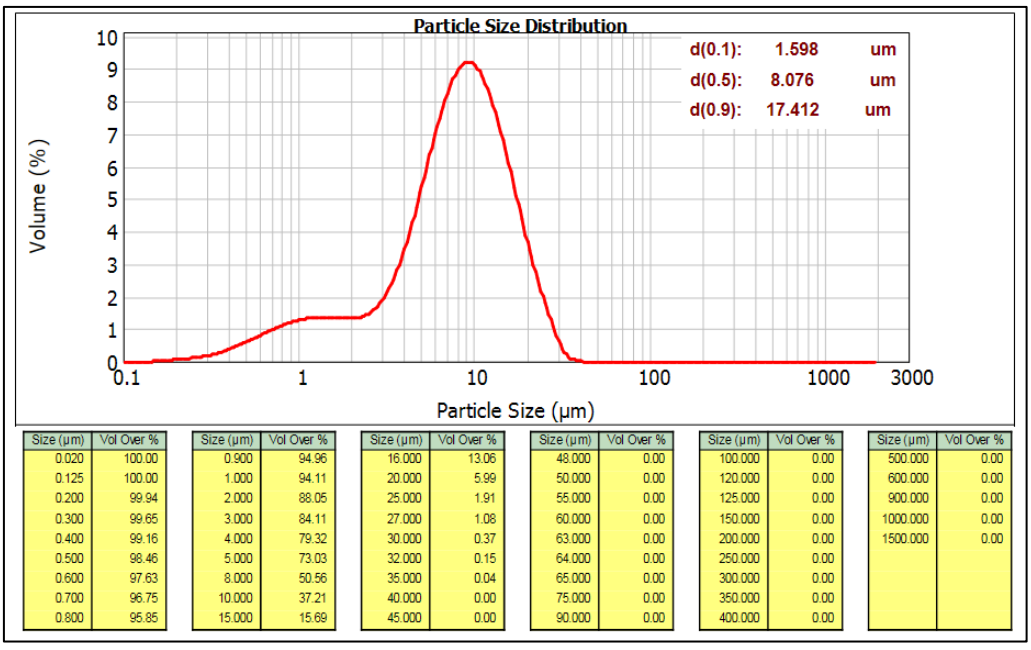

Size (µm)	Vol Over %	Size (µm)	Vol Over %	Size (µm)	Vol Over %	Size (µm)	Vol Over %	Size (µm)	Vol Over %	Size (µm)	Vol Over %
0.020	100.00	0.900	94.96	16.000	13.06	48.000	0.00	100.000	0.00	500.000	0.00
0.125	100.00	1.000	94.11	20.000	5.99	50.000	0.00	120.000	0.00	600.000	0.00
0.200	99.94	2.000	88.05	25.000	1.91	55.000	0.00	125.000	0.00	900.000	0.00
0.300	99.65	3.000	84.11	27.000	1.08	60.000	0.00	150.000	0.00	1000.000	0.00
0.400	99.16	4.000	79.32	30.000	0.37	63.000	0.00	200.000	0.00	1500.000	0.00
0.500	98.46	5.000	73.03	32.000	0.15	64.000	0.00	250.000	0.00		
0.600	97.63	8.000	50.56	35.000	0.04	65.000	0.00	300.000	0.00		
0.700	96.75	10.000	37.21	40.000	0.00	75.000	0.00	350.000	0.00		
0.800	95.85	15.000	15.69	45.000	0.00	90.000	0.00	400.000	0.00		

Figure C.2 The result of particle size analysis of PCC product (limestone origin) produced by using 5% $Ca(OH)_2$ concentration at 10 bar CO_2 pressure

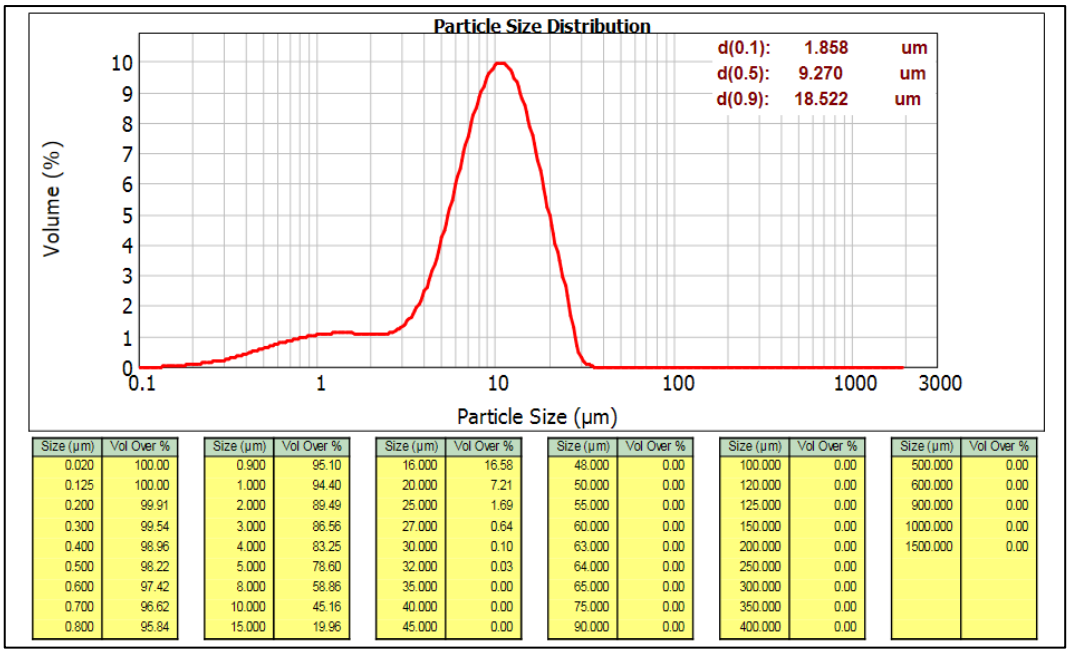

Size (µm)	Vol Over %	Size (µm)	Vol Over %	Size (µm)	Vol Over %	Size (µm)	Vol Over %	Size (µm)	Vol Over %	Size (µm)	Vol Over %
0.020	100.00	0.900	95.10	16.000	16.58	48.000	0.00	100.000	0.00	500.000	0.00
0.125	100.00	1.000	94.40	20.000	7.21	50.000	0.00	120.000	0.00	600.000	0.00
0.200	99.91	2.000	89.49	25.000	1.69	55.000	0.00	125.000	0.00	900.000	0.00
0.300	99.54	3.000	86.56	27.000	0.64	60.000	0.00	150.000	0.00	1000.000	0.00
0.400	98.96	4.000	83.25	30.000	0.10	63.000	0.00	200.000	0.00	1500.000	0.00
0.500	98.22	5.000	78.60	32.000	0.03	64.000	0.00	250.000	0.00		
0.600	97.42	8.000	58.86	35.000	0.00	65.000	0.00	300.000	0.00		
0.700	96.62	10.000	45.16	40.000	0.00	75.000	0.00	350.000	0.00		
0.800	95.84	15.000	19.96	45.000	0.00	90.000	0.00	400.000	0.00		

Figure C.3 The result of particle size analysis of PCC product (marble origin) produced by using 10% $Ca(OH)_2$ concentration at 10 bar CO_2 pressure

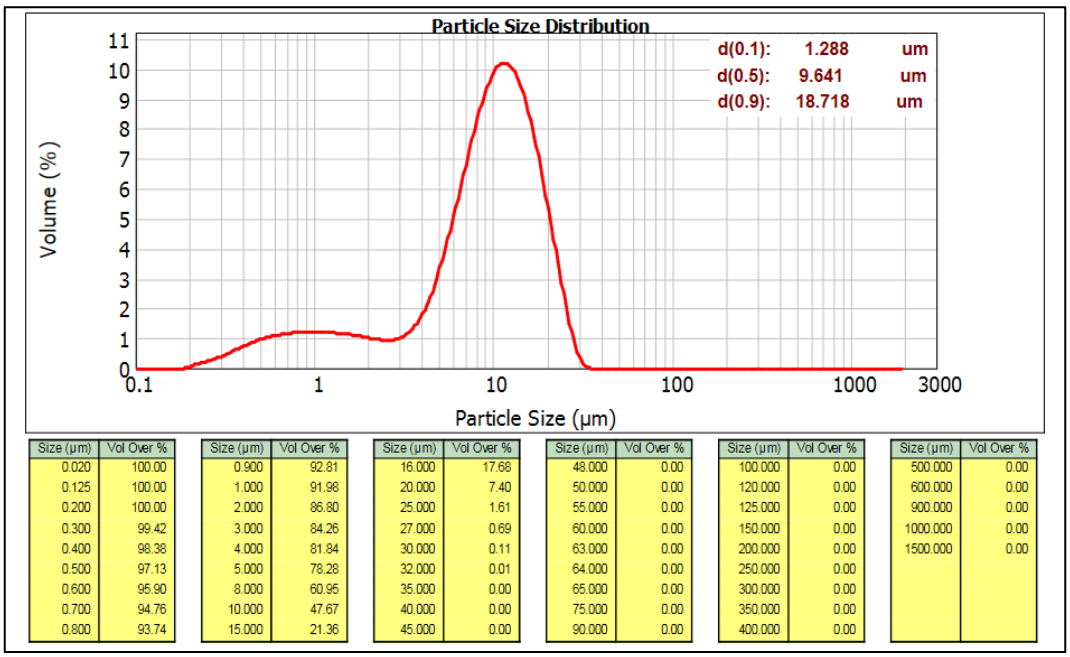

Size (µm)	Vol Over %	Size (µm)	Vol Over %	Size (µm)	Vol Over %	Size (µm)	Vol Over %	Size (µm)	Vol Over %	Size (µm)	Vol Over %
0.020	100.00	0.900	92.81	16.000	17.68	48.000	0.00	100.000	0.00	500.000	0.00
0.125	100.00	1.000	91.98	20.000	7.40	50.000	0.00	120.000	0.00	600.000	0.00
0.200	100.00	2.000	86.80	25.000	1.61	55.000	0.00	125.000	0.00	900.000	0.00
0.300	99.42	3.000	84.26	27.000	0.69	60.000	0.00	150.000	0.00	1000.000	0.00
0.400	98.38	4.000	81.84	30.000	0.11	63.000	0.00	200.000	0.00	1500.000	0.00
0.500	97.13	5.000	78.28	32.000	0.01	64.000	0.00	250.000	0.00		
0.600	95.90	8.000	60.95	35.000	0.00	65.000	0.00	300.000	0.00		
0.700	94.76	10.000	47.67	40.000	0.00	75.000	0.00	350.000	0.00		
0.800	93.74	15.000	21.36	45.000	0.00	90.000	0.00	400.000	0.00		

Figure C.4 The result of particle size analysis of PCC product (limestone origin) produced by using 10% $Ca(OH)_2$ concentration at 10 bar CO_2 pressure

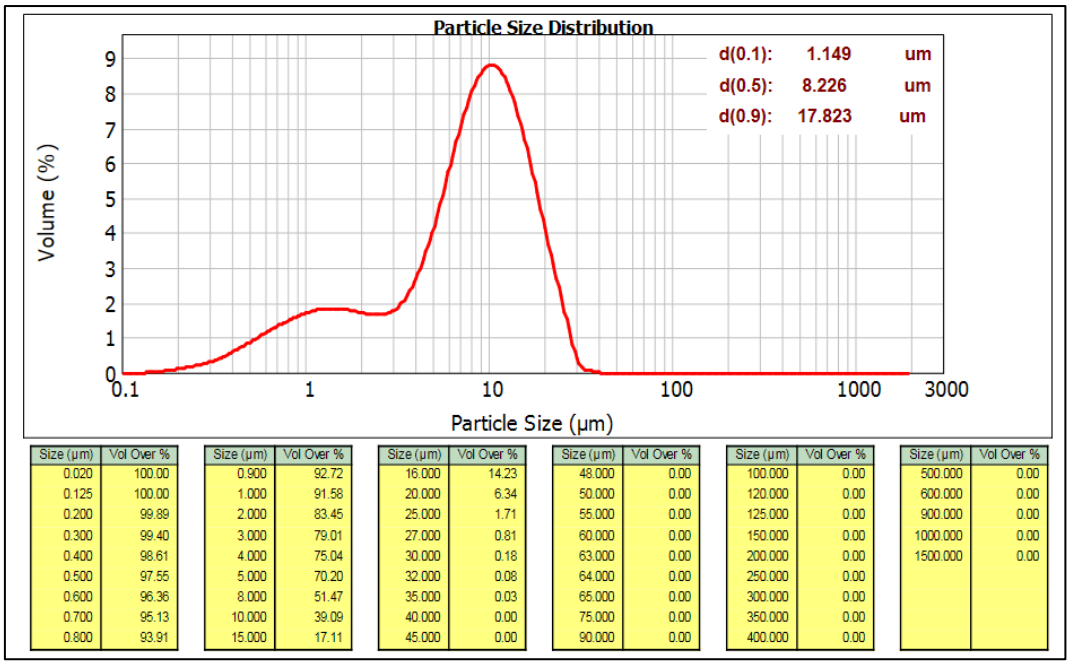

Size (µm)	Vol Over %	Size (µm)	Vol Over %	Size (µm)	Vol Over %	Size (µm)	Vol Over %	Size (µm)	Vol Over %	Size (µm)	Vol Over %
0.020	100.00	0.900	92.72	16.000	14.23	48.000	0.00	100.000	0.00	500.000	0.00
0.125	100.00	1.000	91.58	20.000	6.34	50.000	0.00	120.000	0.00	600.000	0.00
0.200	99.89	2.000	83.45	25.000	1.71	55.000	0.00	125.000	0.00	900.000	0.00
0.300	99.40	3.000	79.01	27.000	0.81	60.000	0.00	150.000	0.00	1000.000	0.00
0.400	98.61	4.000	75.04	30.000	0.18	63.000	0.00	200.000	0.00	1500.000	0.00
0.500	97.55	5.000	70.20	32.000	0.08	64.000	0.00	250.000	0.00		
0.600	96.36	8.000	51.47	35.000	0.03	65.000	0.00	300.000	0.00		
0.700	95.13	10.000	39.09	40.000	0.00	75.000	0.00	350.000	0.00		
0.800	93.91	15.000	17.11	45.000	0.00	90.000	0.00	400.000	0.00		

Figure C.5 The result of particle size analysis of PCC product (marble origin) produced by using 5% $Ca(OH)_2$ concentration at 5 bar CO_2 pressure

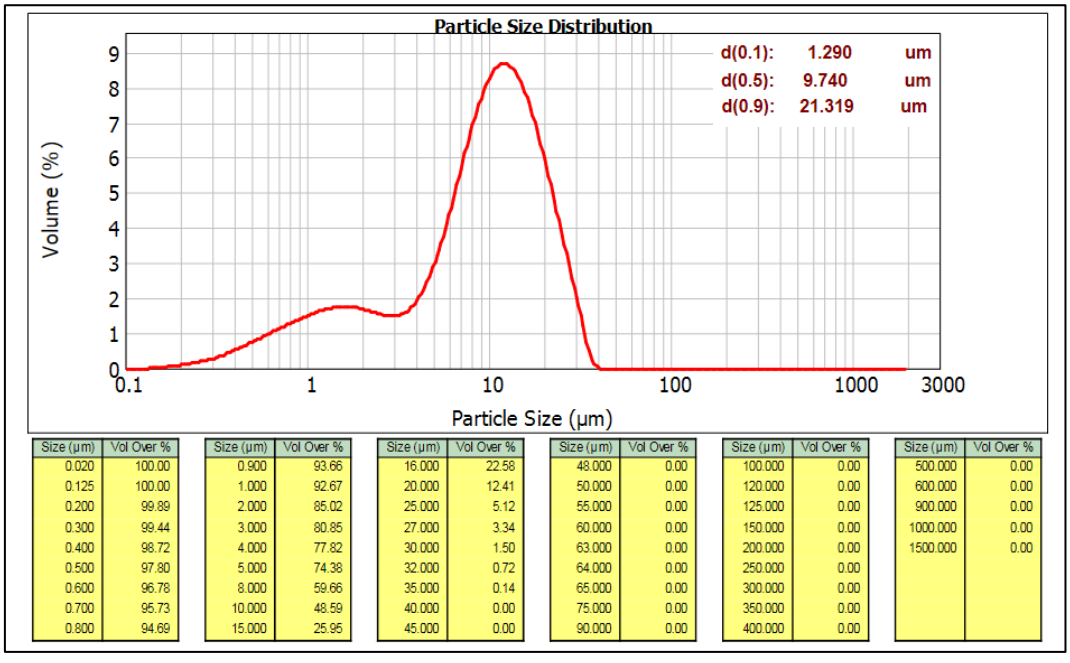

Size (µm)	Vol Over %	Size (µm)	Vol Over %	Size (µm)	Vol Over %	Size (µm)	Vol Over %	Size (µm)	Vol Over %	Size (µm)	Vol Over %
0.020	100.00	0.900	93.66	16.000	22.58	48.000	0.00	100.000	0.00	500.000	0.00
0.125	100.00	1.000	92.67	20.000	12.41	50.000	0.00	120.000	0.00	600.000	0.00
0.200	99.89	2.000	85.02	25.000	5.12	55.000	0.00	125.000	0.00	900.000	0.00
0.300	99.44	3.000	80.85	27.000	3.34	60.000	0.00	150.000	0.00	1000.000	0.00
0.400	98.72	4.000	77.82	30.000	1.50	63.000	0.00	200.000	0.00	1500.000	0.00
0.500	97.80	5.000	74.38	32.000	0.72	64.000	0.00	250.000	0.00		
0.600	96.78	8.000	59.66	35.000	0.14	65.000	0.00	300.000	0.00		
0.700	95.73	10.000	48.59	40.000	0.00	75.000	0.00	350.000	0.00		
0.800	94.69	15.000	25.95	45.000	0.00	90.000	0.00	400.000	0.00		

Figure C.6 The result of particle size analysis of PCC product (limestone origin) produced by using 5% $Ca(OH)_2$ concentration at 5 bar CO_2 pressure

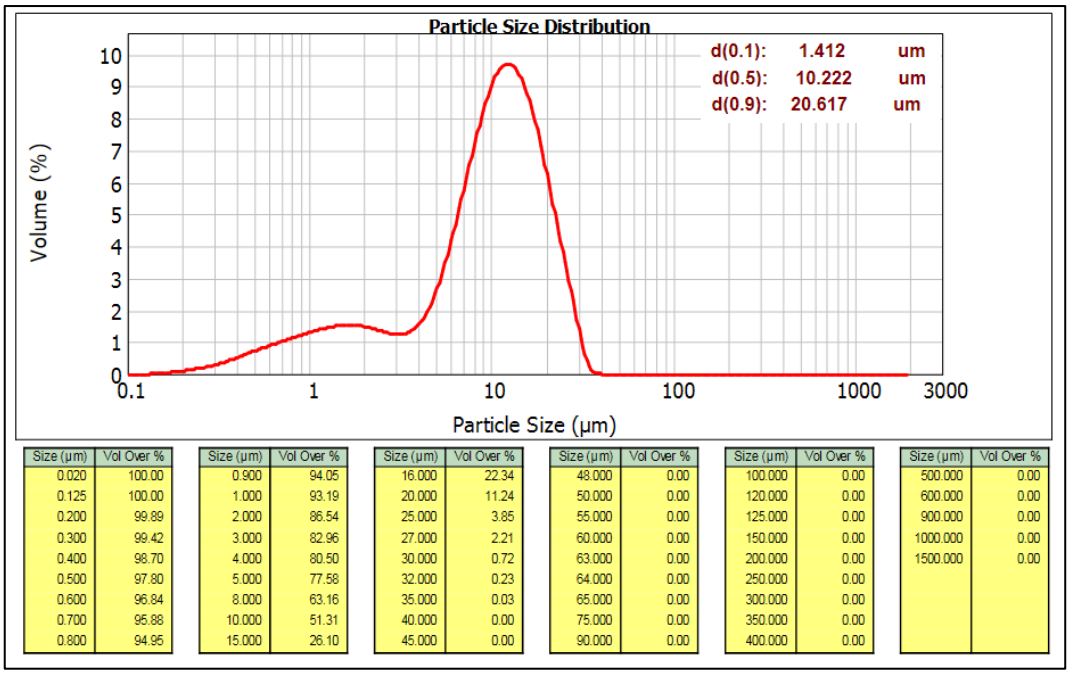

Size (µm)	Vol Over %	Size (µm)	Vol Over %	Size (µm)	Vol Over %	Size (µm)	Vol Over %	Size (µm)	Vol Over %	Size (µm)	Vol Over %
0.020	100.00	0.900	94.05	16.000	22.34	48.000	0.00	100.000	0.00	500.000	0.00
0.125	100.00	1.000	93.19	20.000	11.24	50.000	0.00	120.000	0.00	600.000	0.00
0.200	99.89	2.000	86.54	25.000	3.85	55.000	0.00	125.000	0.00	900.000	0.00
0.300	99.42	3.000	82.96	27.000	2.21	60.000	0.00	150.000	0.00	1000.000	0.00
0.400	98.70	4.000	80.50	30.000	0.72	63.000	0.00	200.000	0.00	1500.000	0.00
0.500	97.80	5.000	77.58	32.000	0.23	64.000	0.00	250.000	0.00		
0.600	96.84	8.000	63.16	35.000	0.03	65.000	0.00	300.000	0.00		
0.700	95.88	10.000	51.31	40.000	0.00	75.000	0.00	350.000	0.00		
0.800	94.95	15.000	26.10	45.000	0.00	90.000	0.00	400.000	0.00		

Figure C.7 The result of particle size analysis of PCC product (marble origin) produced by using 10% $Ca(OH)_2$ concentration at 5 bar CO_2 pressure

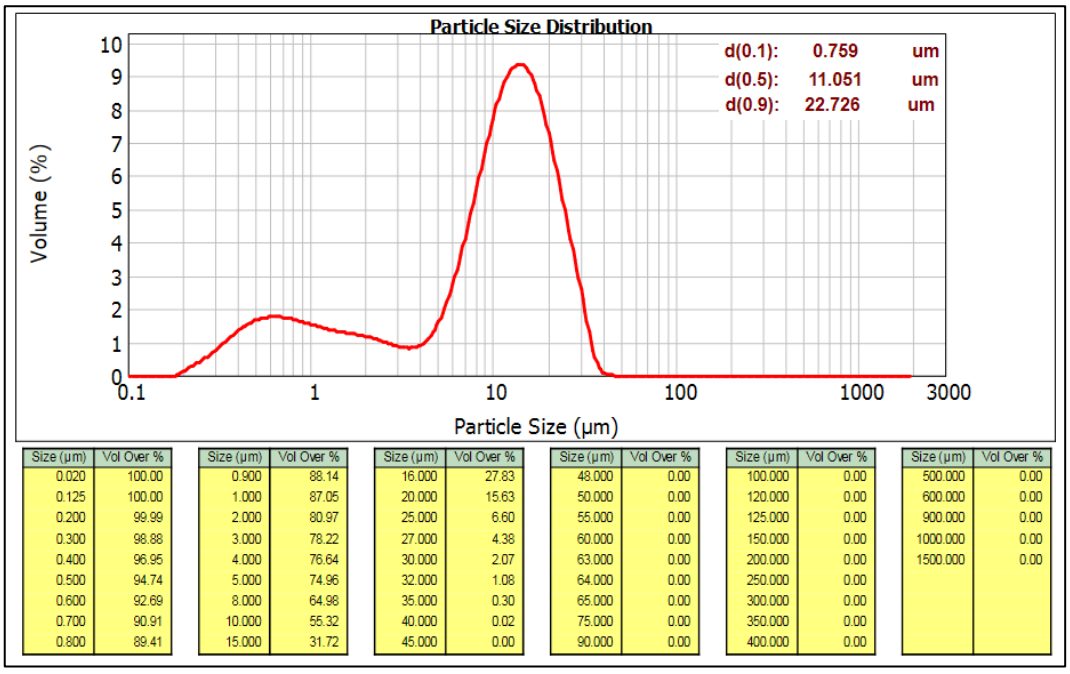

Size (µm)	Vol Over %	Size (µm)	Vol Over %	Size (µm)	Vol Over %	Size (µm)	Vol Over %	Size (µm)	Vol Over %	Size (µm)	Vol Over %
0.020	100.00	0.900	88.14	16.000	27.83	48.000	0.00	100.000	0.00	500.000	0.00
0.125	100.00	1.000	87.05	20.000	15.63	50.000	0.00	120.000	0.00	600.000	0.00
0.200	99.99	2.000	80.97	25.000	6.60	55.000	0.00	125.000	0.00	900.000	0.00
0.300	98.88	3.000	78.22	27.000	4.38	60.000	0.00	150.000	0.00	1000.000	0.00
0.400	96.95	4.000	76.64	30.000	2.07	63.000	0.00	200.000	0.00	1500.000	0.00
0.500	94.74	5.000	74.96	32.000	1.08	64.000	0.00	250.000	0.00		
0.600	92.69	8.000	64.98	35.000	0.30	65.000	0.00	300.000	0.00		
0.700	90.91	10.000	55.32	40.000	0.02	75.000	0.00	350.000	0.00		
0.800	89.41	15.000	31.72	45.000	0.00	90.000	0.00	400.000	0.00		

Figure C.8 The result of particle size analysis of PCC product (limestone origin) produced by using 10% $Ca(OH)_2$ concentration at 5 bar CO_2 pressure

Table C.1 Color results of PCCs produced from marble waste and limestone

	CIE* (X,Y,Z)	CIE* (x,y,z)
PCC produced from marble waste	(85.89, 89.89, 91.45)	(0.321, 0.336, 0.342)
PCC produced from limestone	(91.29, 95.68, 101.72)	(0.316, 0.331, 0.352)
PCC produced by Adaçal Industrial Minerals Co.	(92.77, 97.26, 103.69)	(0.316, 0.331, 0.353)
CIE*: International Commission on Illumination For CIE Yellowness Index: C_x=1.3013, C_z=1.1498 For CIE Whiteness Index: WI,x=800, WI,y=1700, x_n=0.3138, y_n=0.3310		